



Politecnico  
di Torino

# POLITECNICO DI TORINO

Master Degree course in Biomedical Engineering  
Biomedical instrumentation

Master Degree Thesis

## **Ultrasound scanning of inferior vena cava to study the hydration condition during sport**

### **Supervisor**

Prof. Luca Mesin  
Ing. Piero Policastro

### **Candidate**

Ludovico Lattanzio

24 October 2023

# Acknowledgements

I wish to thank the professor Luca Mesin and the engineer Piero Policastro for the expertise and competence that helped guide me through the final part of this journey at times complicated but certainly formative. From dictionary: "formative" is everything that tends to form and develop the intelligence and the personality. Certainly, the Politecnico encloses these values and expresses them through its faculty who help educate students and future professionals capable. So, thanks to all teachers met during the university experience, because each of them, in their way contributed to reach this purpose. Thanks to my special fellow travelers who made the travails lighter through a joke, a laugh and an encouragement. I thank my new companions for their valuable advice. Last but not least, a special thanks to my parents who believed in me, who always supported me, motivated me and who, even in times of difficulty were proud of me by always urging me to believe in the values of study and inviting me to be curious and passionate, albeit in the rigor that the profession imposes

Desidero ringraziare il professor Luca Mesin e l'ingegner Piero Policastro per la perizia e le competenze che mi hanno guidato alla parte finale di questo percorso, a volte difficile ma sicuramente formativo. Formativo, dal dizionario, è tutto ciò che tende a formare e sviluppare l'intelligenza e la personalità. Sicuramente il Politecnico racchiude questi valori e li esplica attraverso i suoi docenti, che contribuiscono ad istruire studenti e futuri professionisti capaci. Pertanto ringrazio tutti i professori incontrati durante l'esperienza universitaria perchè ognuno, a suo modo, ha contribuito al raggiungimento di questo obiettivo. Ringrazio i miei compagni di viaggio Nicolas, Lorenzo, Jacopo che hanno reso più leggere le fatiche attraverso una battuta, una risata e un incoraggiamento. Ringrazio i nuovi compagni Eleonora e Francesco per i preziosi consigli. Ultimo ma non ultimo un ringraziamento speciale ai miei genitori che hanno creduto in me, che mi hanno sempre sostenuto, motivato e che, anche nei momenti di difficoltà, sono stati orgogliosi di me esortandomi sempre a credere nei valori dello studio e invitandomi ad essere curioso e appassionato, seppur nel rigore che la professione impone.

## **Abstract**

Water is essential for our body: more than 60% of our weight is made up of liquids. The analysis of fluid loss during sports performance is crucial for an athlete, as intense sweating can cause dehydration. It can lead to worsening of sports performance, cardiovascular fatigue and, if prolonged and in extreme situations, even hyperthermia, failure of the gastrointestinal system, heat cramps and death. Fluid balance, i.e. the optimal ratio between fluid intake and loss, is critical to athlete performance and safety during exercise, especially in extreme environmental conditions such as high-temperature environments. Being able to perform a fluid loss analysis in a short time and with precision is certainly useful to optimize training and physiological recovery. The aim of this master's thesis is therefore to investigate the fluid dynamic response of the athlete after an effort, noting its effects on the IVC. Currently, methods are used that require long processing times and, consequently, also lengthen the time to know the results, making timely intervention impossible. The ultrasound analysis of the inferior vena cava (IVC), on the other hand, is immediate and allows to verify in real time the volume status of the sports subject, providing an estimate of the hydration status. The main objective of the project is precisely to study the level of hydration of athletes during sports activities and during recovery, to monitor them and improve their performance through real-time control of the diameter of the IVC, using a portable ultrasound probe and a segmentation software owned by Viper s.r.l. To this end, some candidates were subjected to sweating activity. In detail, the dataset is composed of 21 subjects, 9 women and 12 men, and contains healthy subjects differentiated into sportsmen (14) and non-athletes (7), with an age of  $24 \pm 2$  years and a weight of  $70.3 \pm 11.8$  kg. The test protocol provided for subjecting candidates to a sporting activity, i.e. 4 sloping walks on a treadmill lasting 10 minutes each, with slope and speed parameters varying according to the amount of weight lost. During the activity, a POLAR band was worn for ECG monitoring and ultrasound scans of the IVC were performed to observe the variation in the diameter of the IVC, assuming a reduction during the activity. At the end of the acquisition phase and after obtaining the average diameter in the different frames of the ultrasound video, three parameters were calculated that indicate the collapsibility of the IVC: caval index (CI), respiratory caval index (RCI) and cardiac caval index (CCI). By correlating these parameters

and segmented diameters with initial patient data by means of statistical tests (two-sample t-test, one-way ANOVA, multi-way ANOVA), any significant differences in the dataset were evaluated, but were not highlighted. However, the initial assumption on the diameter trend was respected. During exercise, a gradual reduction in the diameter of the veins was noted, while an increase was observed during hydration. The demonstration of these trends was obtained by interpolation between values using linear regression.

# Contents

<b>1</b>	<b>Introduction</b>	<b>5</b>
1.1	Viper	6
1.2	Who benefits from this analysis	7
1.2.1	Heart failure	8
1.2.2	Hydration level for athletes	8
1.3	Possible future clinical application	9
1.3.1	Real time acquisitions	9
<b>2</b>	<b>Cardiovascular System</b>	<b>10</b>
2.1	Structure of arteries and veins	13
2.1.1	Arteries	14
2.1.2	Veins	14
<b>3</b>	<b>Respiratory system</b>	<b>16</b>
<b>4</b>	<b>Anatomy IVC</b>	<b>20</b>
<b>5</b>	<b>Hydration and body fluid balance</b>	<b>22</b>
<b>6</b>	<b>Ultrasound waves</b>	<b>25</b>
6.1	US reflection	26
<b>7</b>	<b>Echography</b>	<b>28</b>
7.1	Structure of an ultrasound scanner	29
7.1.1	TGC	30
7.1.2	Demodulator and scan converter	30
7.2	US generation and beam geometry	30
7.3	Spatial resolution	31
7.4	Echograph	32
7.5	IVC echography	34
7.6	"Good echography"	38
7.6.1	Artifacts in ultrasound images	39

<b>8</b>	<b>Materials and methods</b>	<b>41</b>
8.1	Ultrasound probe . . . . .	44
8.2	Impedance scale . . . . .	44
8.3	Heart rate sensor Polar H10 . . . . .	45
8.4	Treadmill . . . . .	47
<b>9</b>	<b>Test protocol execution</b>	<b>48</b>
9.1	Dataset Costruction . . . . .	49
<b>10</b>	<b>Processing</b>	<b>51</b>
10.1	Segmentation of the vein . . . . .	52
10.2	Diameter generator . . . . .	53
10.3	Conversion factor . . . . .	54
10.4	Extraction of parameters . . . . .	54
10.5	Normalization of diameters . . . . .	54
<b>11</b>	<b>Results and graphs</b>	<b>56</b>
11.1	Statistical test . . . . .	60
11.2	Conclusions . . . . .	63
	<b>Bibliography</b>	<b>64</b>
	<b>List of Tables</b>	<b>67</b>
	<b>List of Figures</b>	<b>68</b>

# Chapter 1

## Intro

The inferior vena cava is the object of analysis in several diagnoses because it can provide important information related to the patient's volemic status, hydration, or blood pressure (right atrial pressure: RAP). This clinical information can be assessed by studying the parameters of the vena cava, among the main ones we include the caval index, or collapsibility index (CI), which provides information about how much the IVC dilates or shrinks. These indexes are calculated using the different diameter observed in respiratory cycle. In particular, the ratio of the maximum diameter to the minimum diameter is exploited for the calculation of CI as follow:

$$\frac{D_{max} - D_{min}}{D_{max}} \quad (1.1)$$

To calculate the above parameters, it is necessary to start by measuring the diameter of the vena cava. This operation it is complicated by three main factors:

- Geometry: along its course the IVC has irregular edges
- Movements: cardiac pulsatility and respiratory movements make difficult to detect the vein , even causing overlap of tissues.
- Repeatability : the ultrasound exam which is used to observe IVC exploits the echo-graphic probe, this promotes intra-operator or inter-operator variability.

Hence, these aspects can complicated diameter detection and consequently make it difficult for clinicians to provide an accurate diagnosis. In this way was developed the VIPER software, which acts on reduction of errors thanks to the automatic measurement of the IVC diameter, both

in longitudinal and transversal section. The software is able to segment the vein, namely to follow the changing of the diameter during time, to obtain a precise measure in each instant of time; the work of the software relieves that of the clinician, who is now able to base his diagnoses on stable and reliable readings.

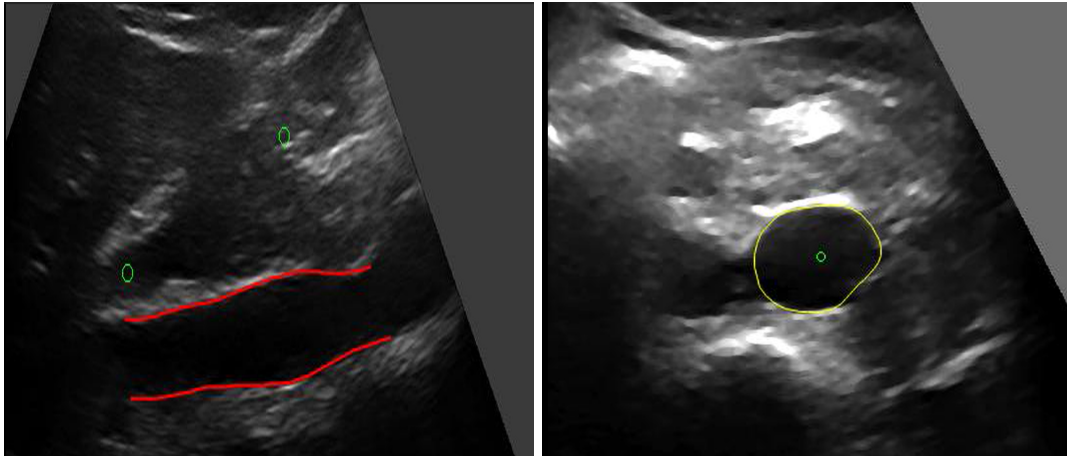


Figure 1.1. *The two segmentations of the IVC: longitudinal(L)and transversal(R)*

## 1.1 Viper



Figure 1.2. [1]

Vein Image Processing for edge rendering in short VIPER is a research project realized in cooperation with Politecnico of Turin. The study aims to rigorously segment the diameter of the inferior vena cava. This work stems from the need to provide the clinical practitioner with a diagnostic tool that is reliable, accurate and such that approximations are minimized. If in the traditional method the CI is measured manually and qualitatively, in the algorithm developed by VIPER it is possible to obtain continuous variations of the caval index over time, which are no longer based on the clinician's manual dexterity but on the automatically segmented diameter that therefore also takes into account geometric factors. [1] In this way, the information contained in ultrasound scans can be fully exploited for diagnostic purposes to sustain the make decision process. The innovativeness and practical importance of the study enabled VIPER to obtain the patent.

## **1.2 Who benefits from this analysis**

Approximately 10 % of patients who access the emergency room are screened for hydration condition, using ultrasound study of the pulsatility of the IVC, in order to better diagnostic-therapeutic framing [1]. First of all, through the software developed by VIPER this percentage of subjects may receive a better diagnosis or even a better monitoring or follow up. Almost 80% of patients that enter in hospital are subjected to fluid monitoring therapy, and so a better and faster treatment is necessary. Secondly, also all the patients who are undergoing ultrasound in the abdominal body region, to analyze the inferior cave vein could obtain an accurate treatment. The lose of body liquids or electrolytes in general is a "consequence of thermo-regulatory sweating during exercise" [9], so the study turns out to be of particular interest in sports where intensive sweating can cause dehydration. Dehydration causes cardiovascular fatigue and if prolonged, in extreme situations even hyperthermia, failure of the gastrointestinal system, heat cramps, and death. Fluid balance, i.e., the optimal ratio of fluid intake to losses, is critical to athlete performance and safety during exercise, especially in hot environmental conditions. Currently, the methods used to determine dehydration states are body weight measurement and urinalysis; both methods are not very immediate with risk of late intervention. In contrast, inferior vena cava analysis could provide a rapid method of analysis that can be implemented on-site, so as to optimize intervention time and avoid the major risks associated with dehydration. So in

brief these two categories get a benefit:

- Patients who enter in emergency department.
- Athletes and sportsperson to keep the body's hydration level controlled.

If for the second category of people, the analysis of the inferior vena cava is limited to the treatment of the subject's hydration status, for people entering the emergency room the edge-to-edge analysis algorithm could be an aid for those suffering from heart failure. In fact, it is possible to hypothesize that the above algorithm could be a concrete aid to health care professionals in improving and optimizing treatment toward patients with heart failure, adjusting the amount of diuretics [8]. This hypothesis is in the context of the need for treatment to cope with the increasing number of patients "are admitted to cardiology departments for the relapse of HF each year". [10].

## 1.2.1 Heart failure

The previous section mentioned the usefulness of ultrasound of the inferior vena cava for heart failure patients. In short, this pathology involves an insufficient venous return to the right atrium of the heart. The percentage of population affected by this issue is almost 1-2%, so it is a common problem [12]. This is the context of a study that established ultrasound analysis of the inferior vena cava caval index as an effective tool for the follow-up of subjects with chronic heart failure. Indeed, through a statistical analysis of the IVC CI, it is possible to identify subjects at risk of worsening health status or hospitalisation [13].

## 1.2.2 Hydration level for athletes

Actually, there are no specific studies to monitor the sweating status of athletes during sport in a controlled and accurate manner. There is one study that monitors the sporting activity of some football players over the long term. [31]. In our investigation, the aim is to scrupulously analyse in detail the small changes in the diameter of the vena cava, in successive measurements not far apart in time, and thus observe significant changes in this parameter that could open the door to a study with possibly real-time measurements during physical exertion

## 1.3 Possible future clinical application

It is expected that our results may have spin-offs to sports medicine, extending in that area the ultrasound study of the inferior vena cava, which, on the other hand, already has clinical applications in various departments (e.g., internal medicine, emergency room, cardiology) where different patients may show very marked differences in volemic status.

The automatic processing of ultrasound scans using algorithms developed by Viper (a spin-off of ETH) allows for greater accuracy in assessing volemic status. This will make it possible to reliably measure even small changes induced by sweating loss of a low amount of fluid during sports activity, providing a useful tool for monitoring the athlete during training. Certainly the future implications of this study are aimed at further investigating the stability and robustness of the results of the edge-to-edge tracking of IVC algorithm, especially as applied to the healthcare field ; providing an increasingly accurate estimate of the vena cava diameter and collapsibility index, to correlate this factor with heart failure and hemodialysis. [8]

### 1.3.1 Real time acquisitions

According to what has been discussed in subsection 1.2.2, the main purpose for the future is to develop a vein segmentation which trace directly the diameter during the acquisition with the US probe. In the previous studies the single frame of IVC scanner are studied. However, to be able to acquire real time ultrasound scans by extracting the parameters of interest, could be useful to separate the cardiac and respiratory components [24] [23]. "The asynchronous summation of the two components introduces variability" [23]. In fact, CI is influenced by the cardiac and respiratory rhythm.

# Chapter 2

## Cardiovascular System

The circulatory system is formed by a network of channels of different calibre, the vessels, in which circulate the blood and the lymph. A distinction is therefore made between a blood circulatory system and a lymphatic circulatory system. The first is the one we are interested in, and it is composed of the heart, arteries, capillaries, and veins. This system is a closed circuit in which the blood is pushed from the heart into vessels with a centrifugal course, the arteries, which, branching out and gradually reducing in calibre, resolve themselves, inside the organs, into very thin vessels, the capillaries [32]. From these are formed the veins, with a centripetal course, which bring back the blood to the heart.

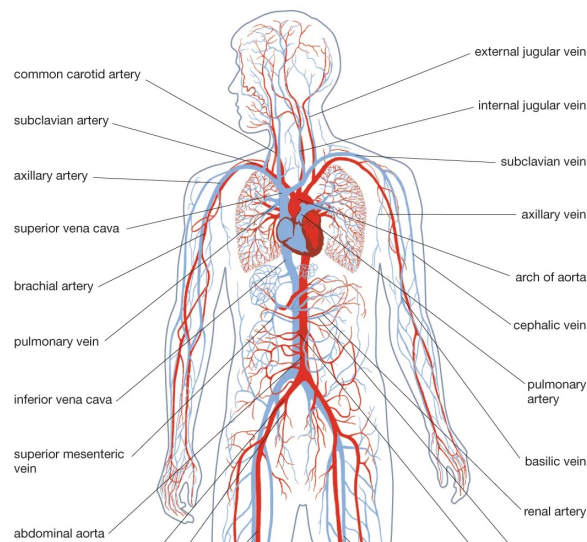


Figure 2.1. *The figure shows the circulatory system and its major vessels*

The heart is divided into right heart and left heart, two independent halves, and each of these are formed by a superior cavity, the atrium, and an inferior cavity, the ventricle. Atria and ventricles communicate through an atrioventricular valve. The two atria are headed by veins, and from each ventricle, through semi-lunar valves, a large arterial vessel departs. The blood circulatory system is then divided into great circulation (general circulation), that originates from the left side of the heart, and small circulation (pulmonary circulation), that originates from the right side of the heart. The great circulation begins in the left ventricle with the aorta, an arterial trunk. The arterial blood, as it passes through the capillary networks that join the arteries to the veins, supplies metabolites and oxygen and is loaded with catabolites and carbon dioxide [32]. In this way, the blood changes from arterial to venous, with a darker colour. The venous blood, via venous branches, the most important of which are the hollow veins, superior and inferior, returns to the heart. The venous trunks flow into the right atrium from which then the blood passes into the right ventricle. The small circulation begins in this ventricle with the pulmonary trunk, which bifurcates and carries venous blood to the two lungs. These branches arrive at a capillary network located on the surface of the pulmonary alveoli walls. The venous blood, passing through this network, gives up carbon dioxide to the atmospheric air and takes in oxygen; having thus become arterial, the blood returns to the heart through the pulmonary veins, which carry it to the left atrium [32]. Then it passes into the left ventricle and the circle starts again. Blood pressure regulates blood flow and is therefore essential for maintaining the body's homeostasis [27]. The mean systemic pressure (MSP) is the pressure that the blood has within the entire cardiovascular system with a stopped heart. Two conditions are necessary to the heart to permit blood circulation:

- A MSP bigger than zero;
- Stretchable vessels.

The first condition is always verified because the system contains an excess of blood volume, and the value of the MSP is about 7 mmHg [32]. The heart is a volume and pressure divider because, by pulsating, it moves blood from the venous to the arterial district, decreasing the pressure in the former and increasing it in the latter. In the left ventricle, the pressure has systolic-diastolic fluctuations from 0 to 120 mmHg. In the arteries, the oscillations have a reduced amplitude because their diastolic value is 70–80 mmHg due to the presence of the aortic valve and peripheral resistances [20]. Instead, due to the lower pre- and

post-capillary resistances, in pulmonary circulation the pressure values are lower than in the general circulation. These resistances low values also allow the pressure to remain pulsatile in the alveolar capillaries. Some important parameters for defining blood pressure values are: cardiac output (CO) defined as the amount of blood pumped by the heart per minute, peripheral resistance (PR) which is the total resistance that opposes blood flow, and mean arterial pressure (MAP) which turns out to be the average between diastolic and systolic pressure in the aorta. The MAP is proportional to the product between the first two values according to the following relationship:

$$CO = \frac{MAP}{PR} \quad (2.1)$$

Each vessel can be assigned its own pressure, called transmural pressure  $P_{tm}$ , which is the difference between pressure in and out of it, and its changes cause variations in the very size of veins and arteries. The following curve shows volume-pressure trend, which is not linear, and describe the link between vascular size and  $P_{tm}$ . according to which

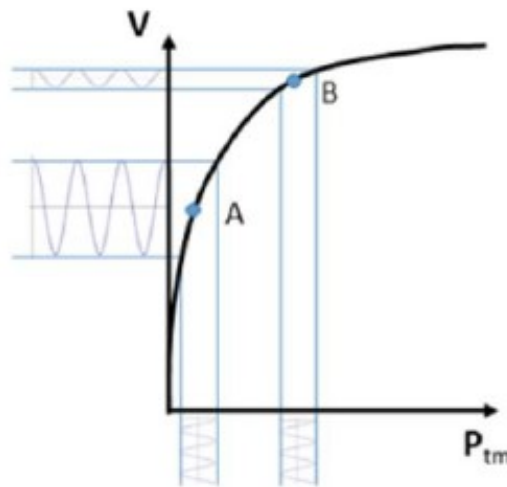


Figure 2.2. Curve volume-pressure [21]

vascular size increases as transmural pressure increases. In arteries, transmural pressure is influenced by the pulse nature of the heart pump and peripheral resistances, whereas in veins, which are characterized

by lower internal pressure, it is influenced by changes in external pressure. Vessel compliance ( $C$ ) is defined by the slope of the volume-pressure curve:

$$C = \frac{DV}{DP_{tm}} \quad (2.2)$$

The curve tends to flatten at high  $P_{tm}$ . We can therefore observe that a change in Figure 2.2: Here is shown the volume-pressure curve. [21]  $P_{tm}$  will also result in a change in vessel volume. If the mean  $P_{tm}$  is high, as in arteries, the vessels size will be larger and the phase changes will be small, but if it turns out to be low we will have larger caliber changes. In other words, when measuring changes in vessel volume in response to given variations in blood pressure, we are assessing the total compliance ( $C_{tot}$ ), which accounts for the vascular ( $C_v$ ) and extravascular ( $C_{ev}$ ) compliance according to the formula:

$$C_{tot} = \frac{1}{\frac{1}{C_v} + \frac{1}{C_{ev}}} \quad (2.3)$$

$C_{tot}$  resulting smaller than  $C_v$  [21].

## 2.1 Structure of arteries and veins

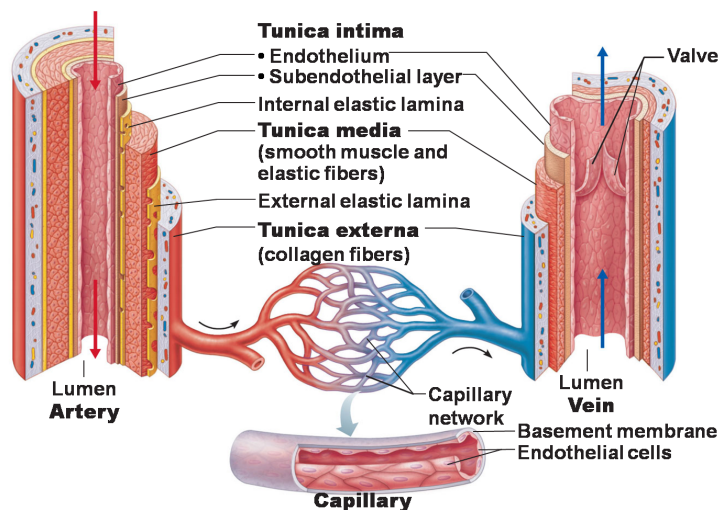


Figure 2.3. Structure of the blood vessels [2]

## 2.1.1 Arteries

Arteries are musculo-membranous conduits lined internally by endothelium. The major arteries are the aorta, from which the arteries of the general circulation are derived, and the pulmonary trunk, which supplies the arteries of the pulmonary circulation. Each artery may give off collateral vessels of a smaller calibre and are often accompanied by one or two veins and one or more nerve trunks; together these formations constitute a vascular bundle. The wall of the arteries consists of three concentric tunics called, from the inside out, intima, media, and adventitia [29]. The media tunica, which is also the thickest, characterises the functional behaviour of the arteries based on its constitution. The media tunica is principally made of muscle tissue in the arteries of small and middle calibre, while it is made of elastic tissue for that of major calibre. So, we can distinguish two types of arteries:

- muscular type: they have contractile walls and can actively vary their lumen regulating the amount of blood flowing to organs;
- elastic type: they have elastic walls and have a passive function in the blood circulation.

Figure 2.3: In that figure are shown the different structure of arteries and veins. Large-calibre arteries are those with a diameter between 3 cm and 7 mm, medium calibre arteries those with a diameter between 7 mm and 2.5 mm and small-calibre arteries and arterioles those with a diameter of less than 2.5 mm.

## 2.1.2 Veins

Veins are membranous ducts, and they originate from the capillary networks of tissues and organs until they converge to form trunks of increasing calibre. They lead the blood returning to the heart from the capillary district to a pressure regime that is considerably lower than that which exists in the arterial tree, a factor of primary importance for their structural characterisation [32]. The main differences between veins and arteries are the following:

- they are easily depressible and dilatable;
- the walls are thinner and less elastic;
- they have valves.

The typical shape of the veins is cylindrical, but when they are empty of blood, they may appear flattened and collapsed. Their number is greater than that of arteries. The overall calibre of the affluent branches is greater than that of the venous trunk that originates from their confluence: the vascular bed is narrowing from the periphery towards the centre and, as a result, the venous current is gaining speed in the direction of the heart [32].

They too, like arteries, are divided into large-, medium- and small-calibre veins. A further distinction is made into superficial and deep veins. The formers are located in the subcutaneous portion, while the latter are found in the muscle interstices and visceral districts. Most veins have valves, pocket-like membranous folds rising from the venous wall with the concavity in the direction of the heart. The distribution of these valves is not regular but correspond to specific functional needs. There are numerous in the districts where the outflow is more difficult, such as in the lower limbs. The walls of the veins, like those of the arteries, are divided into three layers, or tunics: inner (or intima) tunica, media tunica and adventitia (or outer) tunica.

However, in the veins this structural schematization is not constantly applicable and often the boundaries between these tunics are not that evident. The elements composing the veins walls are that also typical of the arteries: endothelium, collagen fibre, elastic fibre, and muscular cells.

The wall of veins differs from that of arteries mainly due to the greater presence of collagen material, that forms the underlying texture, to the disfavour of the elastic contingent. Furthermore, there are several structural differences between the veins themselves. We can, for example, distinguish receptive-type veins with thin walls and propulsive-type veins with thick walls.

# Chapter 3

## Respiratory system

The respiratory system is the anatomic structure that enables the exchange of gases between the body and the external environment. In the specific case the paragraph is referred to the *external respiration* which involved both respiratory and pulmonary systems and ensures a gas exchange between internal blood flux and external air. This means ensuring an oxygen supply of about 250 ml/min [15]. Moreover it has other functions such as: contribute to the regulation of the blood basic-acid equilibrium, permit phonation, participate to the defence against pathogenic factors and external particles in the airways, supply a way to dissipate humidity and heat, increase the venous return and activate some plasmatic proteins when they pass through the pulmonary circulation [29]. To control all the above functions, the respiratory system is composed of several structures (figure 3.1, and the main organs for carrying out respiration are the lungs. Before meeting them, however, air enters the upper airway and enters the trachea. From it begins the conduction zone of which the bronchi and all their branches are part. The last section is the respiratory zone in which the actual exchange between oxygen and carbon dioxide takes place by means of the pulmonary alveoli [15]. Air flow, like blood flow, is a volume flow driven by a pressure gradient, present between alveoli and external air (atmospheric). Air movement depends on this gradient between areas of high pressure and areas of low pressure. When the pressure in the alveoli is lower than atmospheric pressure inspiration occurs, resulting in a pressure gradient that introduces air into them, and vice versa for expiration. The pressure gradients are determined by the respiration muscles that modify the lungs volume. The relation between the pressure and the volume of a gas follows the Boyle law:

$$PV = nRT \quad (3.1)$$

## Respiratory system

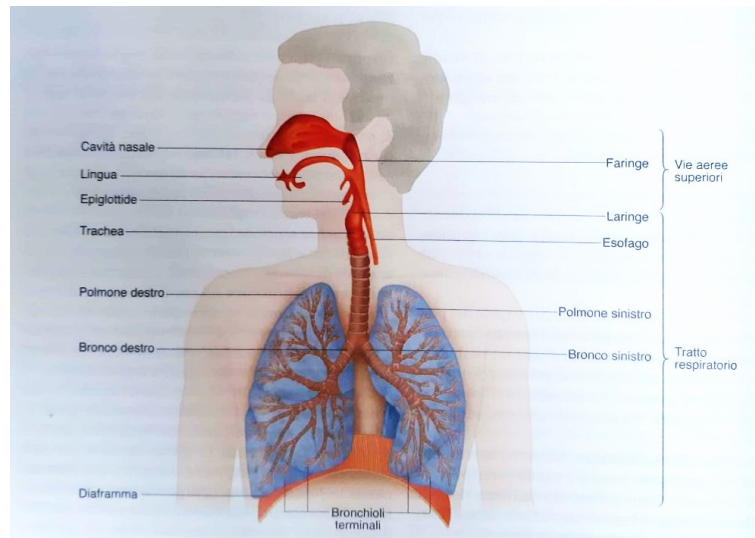


Figure 3.1. Structure of respiratory system. Upper airway and the tract that includes the lungs and the conduction and breathing zones [15]

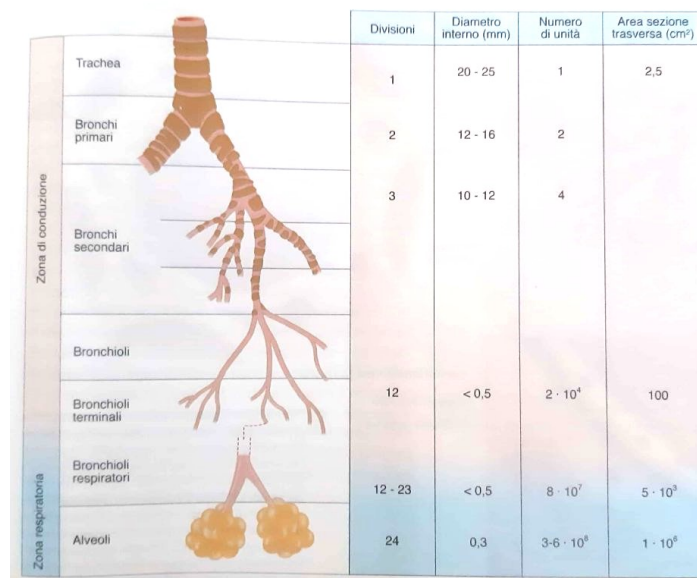


Figure 3.2. Parameters of conduction and respiratory zones [15]

where  $n$  is the number of grams moles of gas,  $P$  is pressure,  $V$  is the volume,  $R$  is the gas constant, and  $T$  is the absolute temperature. The air flow through the lungs is defined as volume flow and its speed is determined by a pressure gradient and a resistance according to the

formula:

$$F = \frac{P_{atm} - P_{alv}}{R} \quad (3.2)$$

where F is the air flow inside the lungs,  $P_{atm}$  is the atmospheric pressure that at sea level is usually 760 mmHg,  $P_{alv}$  is the intra-alveolar pressure that at rest is equal to the atmospheric pressure (thus the differential is 0 mmHg), and R is the resistance to flow.

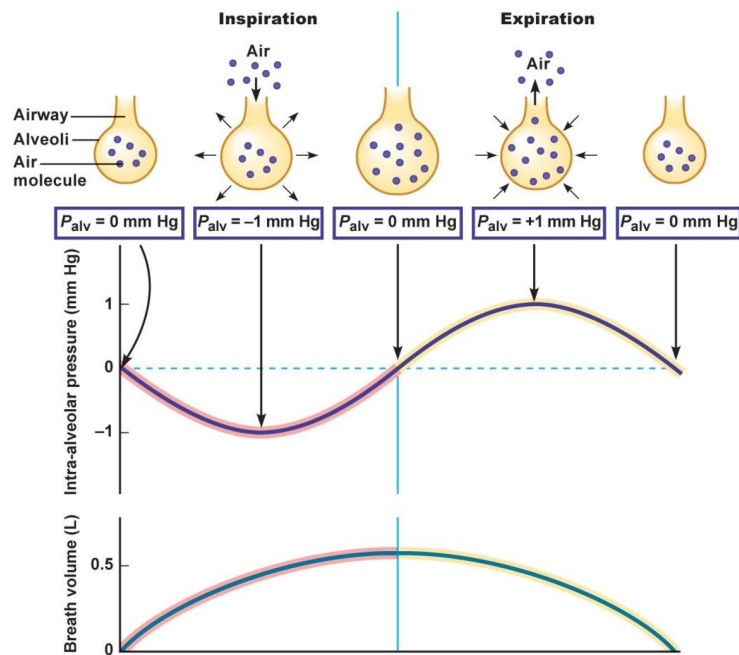


Figure 3.3. The figure shows changes of the intra-alveolar pressure and of the respiratory volume during inspiration and expiration [29]

The inspiratory process begins with nervous stimulation of the inspiratory muscles which causes the thoracic wall to expand and increase its volume. This expansion exerts a pull on the intrapleural fluid, causing a decrease in intrapleural pressure which results in an increase in transpulmonary pressure [29]. As the lungs expand, the pressure in the alveoli drops below the level of atmospheric pressure, so air flows into the alveoli and continues to flow until the pressure reaches the level of atmospheric pressure again. Exhalation, on the other hand, is normally a passive process, not requiring muscle contraction, but only the release of inspiratory muscles. The measure of the facility of the lungs to

expand is called pulmonary compliance (PC), and it is defined as follow:

$$PC = \frac{\Delta V}{\Delta(P_{alv} - P_{ip})} \quad (3.3)$$

Where  $\Delta V$  is the pulmonary volume change, e  $\Delta(P_{alv} - P_{ip})$  is a transpulmonary pressure change. The movement of oxygen and carbon dioxide between the alveolar air and the blood is obtained by diffusion and depends on the concentration gradient. In the alveoli oxygen is in a major concentration and for this reason diffuses into the blood, while carbon dioxide follows the reverse direction.

Oxygen is transported in the blood by haemoglobin, a protein with a special structure that allows oxygen to be bound and released at the right time. Haemoglobin consists of four subunits, each of which contains a globin (globular polypeptide chain) and a heme- group, which contains iron [29]. The bond and release of oxygen is regulated by the  $PO_2$  of the environment that surrounds the haemoglobin. High  $PO_2$  favour the bond of the oxygen with the haemoglobin, while a low  $PO_2$  facilitates the release. The explanation about the respiratory system is useful to introduce the respiratory caval index parameter (RCI), extracted by using a low-pass filter on the signal (diameter) produced over time during the processing of ultrasound videos.

# Chapter 4

## Anatomy IVC

The inferior cave vein (IVC) is a blood vessel of large dimension and its function is to carry the blood from the sub-diaphragmatic body regions to the right atrium of the heart. The cave vein is generated by the union of the iliac veins, located to the right and left of the mid-line. In addition, the cave vein receives as tributaries the lumbar, genital and renal veins. The length of the IVC is about 220 millimeters and it is located on the right side of the body midline.

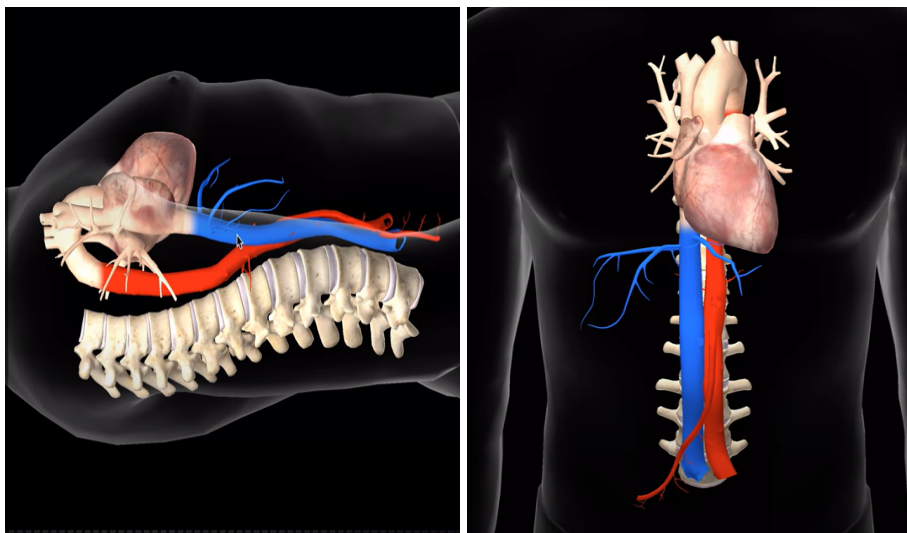


Figure 4.1. *The anatomical position of the IVC from the frontal plane and transversal plane [3]*

The structure of veins, and the vena cava therefore is no exception, is much more deformable than the arteries because the pressure exerted

by deoxygenated blood is lower than the oxygenated blood flowing in the arteries. Wall deformation ensures a lower risk of occlusion, which is one of the greatest risks of damage to the cardiovascular system caused by veins. In fact, the walls of veins, consisting of the tunica intima, media and adventitia, with their collapsibility help the blood flow in different situations, balancing the low pressure.

- the tunica intima consists of the endothelium, a thick subendothelial lamina and sometimes bundles of muscle cells in a longitudinal oblique arrangement;
- the middle tunica is considerably thick and can make up as much as  $2/3$  of the wall and is made up of collagenous bundles and abundant bundles of muscle cells in a circular or spiral arrangement;
- the adventitia tunica is well developed and consists of collagenous connective tissue containing elastic fibres arranged in a network.

“The inferior vena cava is characterized by high compliance, i.e., a good ability to expand elastically under the effect of increasing blood pressure” and then shrink by returning the accumulated blood volume under the effect of decreasing blood pressure [27]. As described earlier transmural pressure changes affect vessel size, and the vena cava is no exception. These pressure changes are regularly produced by the cardiac and respiratory cycles and consequently cause IVC movements in the Longitudinal and transverse planes during breathing. In an ultrasound scan it might be difficult to distinguish the inferior vena cava from the aorta artery because of their anatomical proximity, especially when performing scans in the abdominal or toracic region. To clearly distinguish these two vessels, it is a good idea to look at just the walls and collapsibility. Knowing that the IVC has much thinner walls that deform by exerting pressure.

# Chapter 5

## Hydration and body fluid balance

Water is the most important defining element of life, and it is essential in our organism. Suffice it to mention that water contributes 50–70% of total body mass and is compartmentalized within intracellular (65%) and extracellular (35%) [33]. Water is essential for its ability to keep in solution the precursors and products of our metabolism, and to allow their transport in the body [28]. Water is also essential to:

- Maintain blood volume.
- Transport nutrients.
- Remove metabolic waste through hepatic and renal way.

For these reasons, a good level of hydration is fundamental to keep the Total Body Water (TBW) content within the right levels and to maintain an optimal state of well-being. It is estimated that to achieve this objective it is necessary to introduce 2–3 L of liquids per day, equal to the amount eliminated daily by the body, mainly for thermoregulation and with urine [28]. If the intake of fluids is not enough or if we are submitted to a prolonged exercise that cause the loss of hypotonic fluid in the form of sweat, the organism can enter a condition of dehydration. Dehydration is typically defined as acute weight loss of 1% to 2% of body weight [31] and it increases cardiovascular strain. In particular, the loss of the 2% of body weight is dangerous for the organism and can provoke different disorders such as cardiovascular strain, hyperthermia, physical performance and concentration reduction, heat cramps and, eventually, death. That is why fluid balance is crucial for the athlete's optimal performance and safety during exercises [33]. Sweating, that increases the dissipation of heat to the environment through evaporative cooling,

can be of only 100 mL/hour during a moderate activity but can go up to 3 L/hour for a prolonged or vigorous exercise in a hot environment. This results in a decrease in total body water volume. Many factors influence the hydration status of the human body:

- Availability of fluids
- Environmental conditions
- Structure of exercise
- Intrinsic factors and sport-specific factors

Average Intake per Day	Average Output per Day
Metabolism, 10%, 250ml	100ml, Faeces, 4%
Foods, 30%, 750ml	200ml, Sweat, 8%
Beverages, 60%, 1500ml	700ml, Insensible loses: skin and lungs, 28%
Total Intake, 2500ml	1500ml, Urine, 60%
	2500ml, Total output

Table 5.1. *Estimation of quantity of fluids lost every day.*

In the athletic setting, hydration status is most often assessed by monitoring weight and urine concentration [31] at the first urination of the morning. When more precision of acute hydration changes is desired, plasma osmolality, isotope dilution, and body mass changes, used in appropriate context, provide for the accurate gradations in measurement often required in research [11]. For urine concentration the markers used to estimate dehydration are a reduced urine volume, a high urine specific gravity (USG), a high urine osmolality (Uosm), and a dark urine colour (Ucol). For the body mass, instead, acute changes in hydration are calculated as the difference between pre- and post-exercise of it (this technique implies that 1 g of lost mass is equivalent to 1 ml of lost water). The level of dehydration is best expressed as a percentage of starting body mass rather than as a percentage of TBW because the latter varies widely [11]. These two methods are simple and non-invasive but also not immediate and rapid. It was therefore thought to exploit the sonographic measurements, a quick and easy method, of the inferior vena cava (IVC). In fact, ultrasound determination of the IVC diameter is a valid marker of volume status and, therefore, hydration in the individual. The venous district can provide useful indications for the assessment of hydration status through the ability of veins to collapse during respiratory dynamics. Static and dynamic observation of

the IVC, the supra-hepatic veins and the jugular veins, provides useful indicators for the estimation of hydration by means of the vessel caval index (CI) obtained from the ratio of the difference between the vessel diameters in the expiratory and inspiratory phases to that of the expiratory phase. In particular, the first two are observable by means of a convex probe (used in this study). Normal values of the caval index are between 0,75 and 0,40: CI values above 0,75 express hyper-hydration, while values below 0,4 indicate dehydration [25].

# Chapter 6

## Ultrasound waves

For the human beings, the audible frequencies are included between 20 and 20k Hz, so sounds over these frequencies are called ultrasound. The ultrasound are mechanical waves, and they need a medium to propagate, they do not propagate in the vacuum. They are described by wave mechanics notations: frequency, intensity, wavelength, amplitude, and propagation speed. Frequency is particularly relevant because it represents a fundamental parameter of the ultrasound probe, as the depth of penetration of the mechanical wave into the tissues is regulated precisely by it. Closely related to the type of tissue crossed by the US is the speed of propagation. In fact, from the following relationship, the propagation velocity can be derived from the very frequency used to penetrate the tissues.

$$v = \lambda * f \quad (6.1)$$

Where  $v$  is the propagation speed,  $f$  is the wave frequency and  $\lambda$  is the wavelength. The wavelength turns out to be a measure of the minimum spatial resolution one must have within an image. The higher the frequency, the better the quality of the image we obtain. In particular, the following equation shows how to obtain the velocity of US in human liquids and tissues:

$$v = \sqrt{(E/\rho)} \quad (6.2)$$

where  $\rho$  is the density of the material, expressed in kilograms per cubic meter and  $E$  is the Young's modulus. For most tissues the velocity varies between 1500-1600 m/s, but the most common value for biological tissues is 1540 m/s, so many instruments are calibrated to it. In some devices optimized for abdominal scanning, a speed of 1550 m/s is used because it is the propagation speed of the liver, the most important and studied organ in the abdomen. In practice, however, no

major differences are observed between scans obtained at 1540 m/s and 1550 m/s.

Tissue	Absorption (dB/MHz cm)
Air	-
Fat	0.5
Muscle	2
Liver	0.7
Brain	1
Compact bone	4-10
Water at 20°C	0.002

Table 6.1. Rate of absorption of tissues

## 6.1 US reflection

The physical law that governs wave's reflection and transmission is the Snell's law.

$$\frac{\sin(\theta_1)}{\sin(\theta_2)} = \frac{v_1}{v_2} = \frac{n_1}{n_2} \quad (6.3)$$

Note that  $\theta_1, \theta_2$  symbolize the angles with the perpendicular direction, which in the figure 6.1 are represented by "i" and "f". The second term of equations instead represents the velocity of propagation of US wave into the two materials crossed by it, and it is equivalent to the ratio of the refractive indices of materials  $n_1, n_2$

What we are interested in is the quantity of ultrasound, which is transmitted into the human tissues, so the refracted waves. The transmission coefficient T give us an estimate of this quantity:

$$T = 1 - R \quad (6.4)$$

where R is the reflection coefficient, obtained with acoustic impedance of the two tissues:

$$R = ((Z_1 - Z_2)/(Z_1 + Z_2))^2 \quad (6.5)$$

The acoustic impedance exploits a measure of how much the anatomical district is permeable by US. A high Z means that US cannot be transmitted over the tissue, but they are reflected in large part. This happened for example in the bones where the US are completely reflected and the echo image appears very brightness, avoiding to look for the

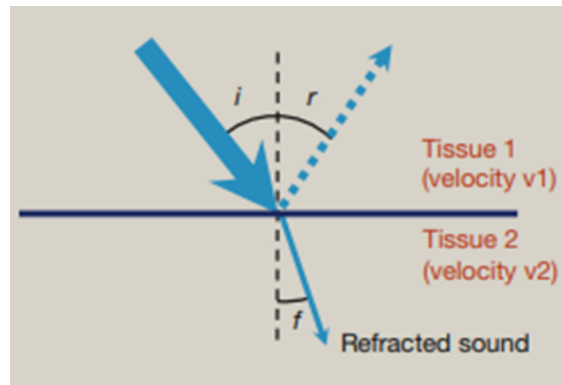


Figure 6.1. The figure describes a wave propagating from material 1 to material 2. At the interface, part of the wave is transmitted to material 2 with different angle ( $f$  angle) and part is reflected ( $r$  angle) at the same angle to the normal [26]

underlying tissues. Taking into account that US propagation velocity on tissues ( $v$ ) is almost 1540 m/s and that with probes it is possible to know *US flight times*  $\Delta t$ , to know the penetration's depth it is sufficient follow this equation:  $d = 1/2 * v * t$

The  $1/2$  factor depends on flight times. As a matter of fact,  $\Delta t$  is the time it takes US to get there and back.

Material	Density ( $kg/m^3$ )	Propagation speed (m/s)	Acoustic impedance ( $kg/m^2/s * 10^6$ )
Air	1.2	330	0.0004
Water	1000	1480	1.48
Media soft tissue	1060	1540	1.63
Liver	1060	1550	1.64
Muscle	1080	1580	1.70
Fat	952	1459	1.38
Brain	994	1560	1.55
Kidney	1038	1560	1.62
Lung	400	650	0.26
Bone	1912	4080	7.80

Table 6.2. Density and acoustic impedance of air, water and biological tissues with propagation rate of US in them.

# Chapter 7

## Echography

The principal medical application of this ultrasound is the ultrasonographic techniques like echography, where the waves exploit the human tissues to propagate and thanks to this spread it is possible to extract some information by the clinical operator. The echography (or ultrasonography) is an imaging technique very widespread in clinical applications due to its easy to use. Contrary to what you might think, although the US passes through the tissues, they are not harmful cause they do not emit ionizing radiation. Moreover, the portability is an advantage because it allows to make measure everywhere, using just a portable probe. Often with this technique it is done "first level analysis" which means investigate some portions of tissues to looking for something suspicious. However, the relative simplicity of the technique hides some disadvantages. Unfortunately, this technique has a low spatial resolution and depends also on the ability of the operator, because to extract some type of information it is necessary to investigate specific portions of tissues with the ultrasound probe, and the region to be monitored are selected by the operator. More you analyse in depth, more you lose in resolution. Knowing that US frequencies goes from 1 to 10 MHz, the probes are set to work in surface after almost over 7MHz (i.e., 7.5 for thyroid) while under these frequencies the probes generate US that penetrate more in depth in the district, losing some spatial resolution. Basing on what it is necessary to observe, the ultrasound allow to acquire signals in three modes:

- A-MODE: amplitude mode. Frequently used in ocular ultrasound, the output signal will be a one-dimensional signal
- B-MODE: brightness mode. The most diffuse technique, repeatable in time with the peculiarity to acquire a single frame per times.

- M-MODE: motion mode. With this mode the probe acquires a dynamic sequence of frames to display a set of images on screen which give the chance to observe what's happen in a determinate real time interval. To analyse vessels this technique is highly recommended.

## 7.1 Structure of an ultrasound scanner

The equipment of an ultrasound scanner is composed by a pulse generator which is the source of US , a probe that emit and receive echoes, and finally a circuit with TGC, demodulator, scan converter and monitor. The most important component is the ultrasound generator. It is always present, and it is a radiofrequency generator which is responsible for generating the electric field at the desired frequency (in this case ultrasound frequency). Synchronized high-voltage pulses are sent to the piezoelectric crystals in the probe. The pulse length determines the axial resolution and usually varies between 0.1-1.1 mm, and there must be enough time between two pulses to allow the return echo to reach the transducer before the new one. The repetition rate of the pulses can be adjusted. There are two types of emission modes: pulsed and continuous. In the second case, the crystals are divided between those that emit and those that receive.

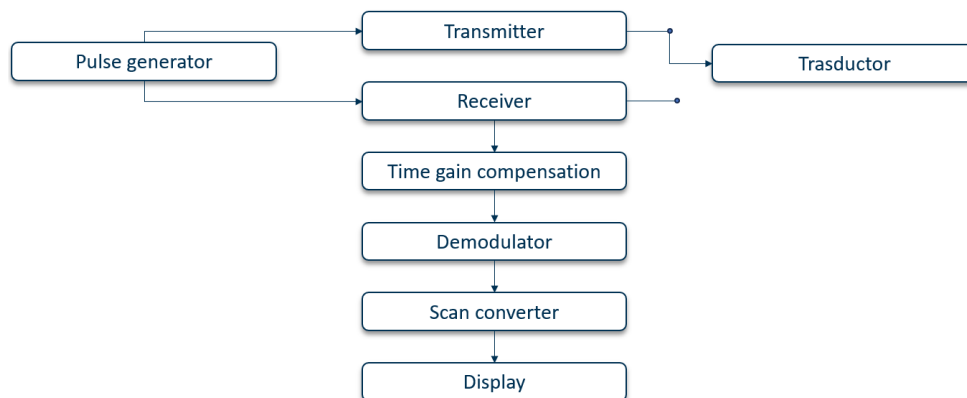


Figure 7.1. *Ultrasound scanner blocks diagram*

### 7.1.1 TGC

When the US propagate and are reflected due to acoustic impedance discontinuity two things happen:

- Reflexion effect: the US pulse finds an area where there is a discontinuity of acoustic impedance, and according to the reflection coefficient some of the energy goes back to the source;
- Tissues attenuation: the US pulse loses intensity with propagation, when it finds a discontinuity, it is reflected and on the return journey it again undergoes attenuation. So, when it reaches the probe, the echo amplitude is not only a function of the reflection coefficient value but also of the attenuation.

The TGC is specifically used to compensate for the depth effect that is superimposed on the effect of the reflection coefficient when an echo arrives at the probe. Its task is then to rebalance the amplitude of the echoes so that it returns to being dependent only on the reflection coefficient. If we want to compensate for the effect of attenuation, that is a decreasing exponential, the amplifier must have a logarithmic law, so the TGC is a logarithmic amplifier that takes time-of-flight as input. In this way shallow echoes are amplified very little and as the echo is deeper and deeper it is amplified more.

### 7.1.2 Demodulator and scan converter

These two blocks basically serve to convert the amplitudes of the received echoes into numerical values and to fill a video matrix that will be the image shown on the monitor. In particular, the demodulator governs the dynamic by which a numerical value is assigned to a given echo amplitude.

## 7.2 US generation and beam geometry

Special materials called piezoelectrics are used to generate ultrasound. these are materials, in the form of crystals, that can transform an electrical quantity into a mechanical quantity and vice versa. the phenomenon of piezoelectricity is divided into two main effects:

- direct piezoelectric effect: a  $\Delta l$  change in the size of the crystal causes a change in  $\Delta V$  potential between the faces of the crystal;

- inverse piezoelectric effect: a  $\Delta V$  change between the potential of the crystal faces causes a compression or  $\Delta l$  expansion of the crystal itself.

In ultrasound devices, therefore, their generation is achieved by piezoelectric crystals by exploiting the inverse piezoelectric effect. The crystals are properly voltage driven and generate a vibration transferred to the patient's tissues by contact. In addition, using the direct piezoelectric effect we can also measure the ultrasounds reflected by the tissues. The mechanic wave reflected hits the sensors, causes their mechanic deformation that becomes a variation of electric potential. Initially quartzes were used as crystals, today a ceramic filled with different elements (phosphorus, zirconium, and titanium) with the following abbreviation is used: PZT. They emphasize the piezoelectric effect and have a longer mechanical durability, but they are fragile, so they need to be treated with care. Geometric dimensions of the crystal are very important because they are related to the frequency generated:

$$f = \frac{2}{h} \quad (7.1)$$

Where  $h$  is the thickness of the plate. Therefore, the smaller the crystal the higher the resonance frequency. In the beam emitted by a single transducer, a proximal zone and a distal zone are identified, in the latter the beam diverges. The extent of the proximal zone is given by:

$$L = \frac{d^2}{4 * \lambda} \quad (7.2)$$

Where  $d$  is the dimension of the crystal,  $L$  is the length of the proximal zone and  $\lambda$  is the wavelength. The beam, in order to be used on ultrasound devices, will be subjected to the focusing process. The zone of maximum focusing is called 'focal area' while the point of maximum collimation is called 'focus'. The beam can be focused through two different techniques: mechanical focusing and dynamic focusing

### 7.3 Spatial resolution

The effective resolution of a US device depends on how the ultrasounds are emitted. Spatial resolution theoretically coincides with the wavelength, but in practice this is not true. A pulse made by several sine cycles exits from a probe. This packet propagates into the tissues; upon encountering a first discontinuity it will be partially reflected and return

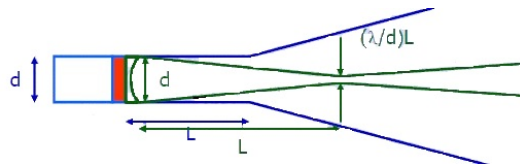


Figure 7.2. The figure shows the geometry of a US beam and demonstrate the necessity of the focusing process.

back to the probe. At a second discontinuity it will be reflected again creating a second packet back to the probe. If the length of this initial packet is less than the distance  $d$  between the two interfaces the packet generated by the first reflection and any packet generated by a second reflection return to the probe at different times. But if this distance is less than the distance  $d$  the two return echoes arrive at the probe overlapping. So, it is the duration of the packet that defines the actual spatial resolution of the device. However, we cannot emit packets that are too short since we would have a return echo with a bandwidth too wide. The compromise is to emit a packet that has a sine wave cycle content ranging from 3 to 5 with some exception. The field of a real probe is placed in a three-dimensional fan. Therefore, there are three resolution directions: axial, lateral and in elevation. For modern probes, however, it is important to have a good axial resolution, that is, the ability to distinguish two objects on the path of the ultrasound moving away from the probe.

## 7.4 Echograph

The ultrasound probe is the instrument that transforms electrical energy into mechanical energy, in the form precisely of ultrasound waves, and vice versa. Because of this characteristic it is called a duplex transducer. The most important part are the piezoelectric crystals whose properties, described above, allow precisely the phenomenon of energy transformation. They, inside the probe, are protected and isolated acoustically and electrically by encapsulation in a matrix of epoxy resin or other similar material. Modern probes consist of array of sensors that can have different geometric arrangements. There are four different types of probes:

- Linear array probes: crystals are arranged along a line. These probes have the highest number of crystals, from a minimum of 128 to

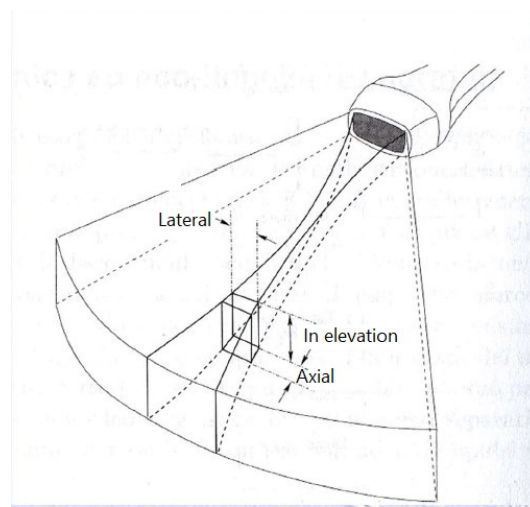


Figure 7.3. The figure shows the field of a real probe and its three resolution directions: axial, lateral and in elevation.

a maximum of 256. Linear probes are suitable for surface applications and thus for the investigation of what is 3 to 4 cm below the skin, but with a very high resolution. They are high frequency probes with a typical range of 5 up to 15 MHz. They have the disadvantage of requiring a large contact area with the skin, so they are not suitable for sub-sternal or intercostal ultrasound.

- Convex array probes: crystals are arranged along a curve. Typically, the ray of curvature is 60 mm and they have a number of crystals which goes from 100 to 120. The frequency range is smaller, from 2 to 7 MHz, because the emission frequency of the probe is lowered to reduce the attenuation imposed by the tissues. The acoustic field fans out in depth, basically it widens as it propagates, and it is therefore possible to observe a relevant portion of organs and tissues at the same time. The investigation depth is of 15–20 cm and for these reasons this is the election probe for abdominal organ scans, thoracic and abdominal tract vascular type scans, and obstetrics and gynaecology scans.
- Phased array probes: they can steer the beam as desired by appropriately driving the crystals. The probe has a small support base but can generate a beam in every direction. It has three main applications, that is, the transthoracic echography, the transcranial echography and the paediatric field.

- Microconvex probes: they are invasive probes, have a shape that fits the investigation done from the inside and are called cavitory probes. Every cavitory probe is a convex probe, that is, the emitted field is always divergent in a larger or smaller fan-shaped pattern depending on the organ to be investigated. The frequency can be raised, 4-10 MHz, because we have less tissue to go through.



Figure 7.4. *The probe used for the acquisitions [4]*

## 7.5 IVC echography

When an IVC echo is performed, the user investigate a treat of body of almost 20 centimeter, placing the probe on the right of the body mid-line, just under the rib cage to see the last part of right atrium and the initial treat of the IVC. The vein continue until the sub diaphragmatic zone. In addition, in order to execute an optimal ultrasound acquisition, the use of gel is essential to limit the formation of shadow zones, but especially to avoid the presence of air between tissue and probe, which would impair the visibility of the ultrasound image. From the point of view of mechanical execution, two cases can be distinguished:

- TRANSVERSAL SECTION, in which the probe was oriented with the highlighted point in figure toward the mid-line;
- LONGITUDINAL SECTION, in which the same point was oriented upward, in the head direction.

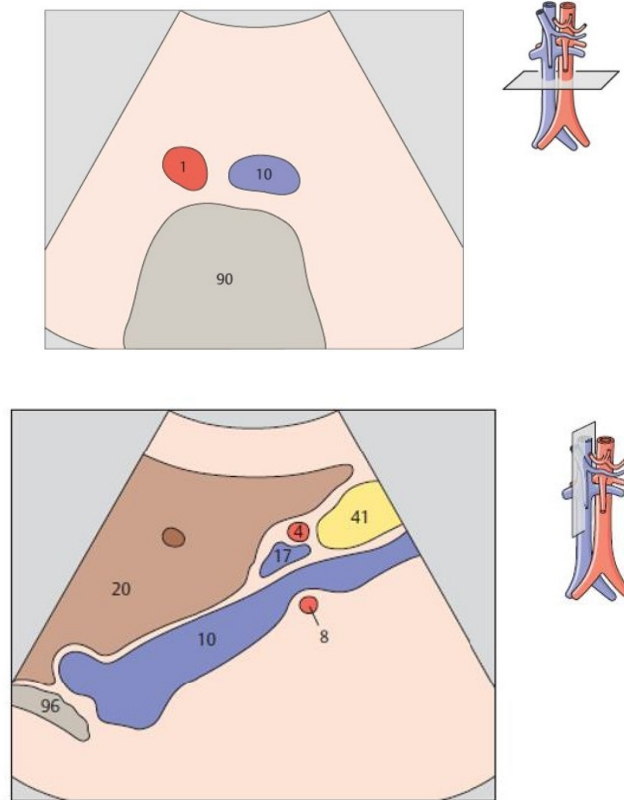


Figure 7.5. The images show the orientation of vein according to our probe position [5]

The IVC is indicated with the number 10 in figure. The output of the veins in the figure is justified by the position of the probe. This happens because it is possible to understand the physiological orientation of the body regions being investigated with the ultrasound scan thanks to the indicator on the left side of the probe.



The same calibration operation was carried out for the longitudinal axis of the vein, orienting the indicator in the cranio-caudal direction. Starting from the short axis view, with a 90 degrees rotation was observed the IVC in longitudinal axis.

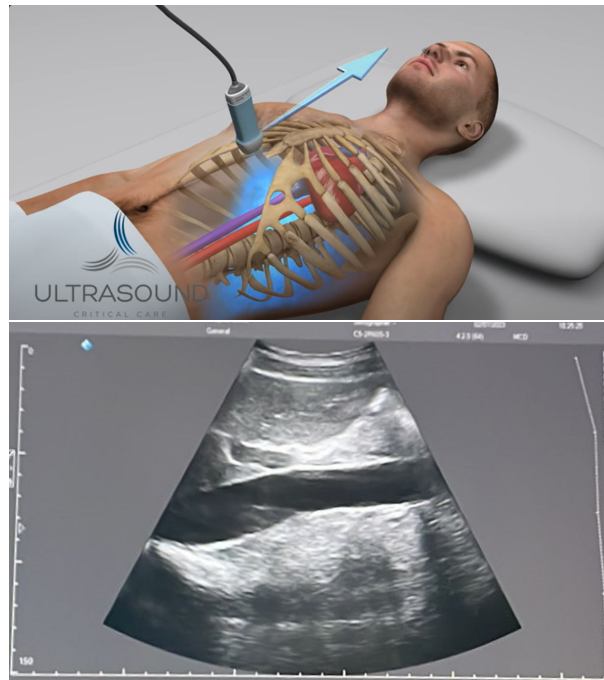


Figure 7.7. The upper image [6] show the indicator orientation cranio-caudal direction. The lower image highlights the correspondence of indicator with the body region visualised on display

## 7.6 "Good echography"

When we acquire echographic images they could be affected by noise or tissues overlap, these factors contributes to increase the quantity of elements that are acquired during an echographic scan. To reduce these factors, in order to have an echo which is easy to read, make the scan a qualitative scan. So the quality of an echographic video is measurable with the ease of instantly and unambiguously recognizing the item or the items of interest.

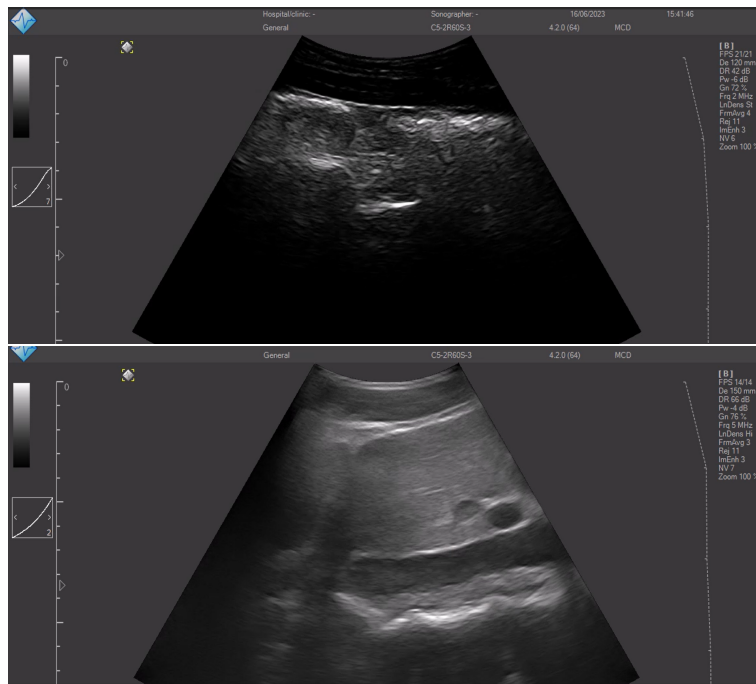


Figure 7.8. Two acquisitions with SW by Telemed [16]

Ultrasound images acquired with portable probes are basically less qualitative than images obtained using fixed hospital ultrasound machines. Furthermore, it is the clinician's experience that enriches the quality of the image or video. Portable probes with versatile characteristics have been available on the market in recent years and therefore allow clear images to be obtained (where it is clearly evident what the user wants to identify) even if the hand of the person using the instrument is not so expert. The good quality of an echographic exam can also be seen from the clinician's ability to interpret the results obtained [14].

### 7.6.1 Artifacts in ultrasound images

Overall, to obtain a "good echography" one of the key passages is to avoid artifacts, in order to have a clean image. Artifacts arise because assumptions are made about the physics of the US that are not always met, thus going to create a sliding between reality and the physical modelling exploited. Sometimes instead they are generated by functional or structural malfunctions and problems and they are called *motion artifacts*". We can group the artifacts into four macro groups based on the assumptions made:

- Boundary shadows: it is caused by the reflection and refraction of the US beam.
- Reverberation: it occurs at a wide and highly reflective areas. Part of the US wave is reflected and starts to oscillate between the hyper-reflective walls of two structures. The echoes received from the transducer at different times and with different intensities, due to multiple reflections, give a false information about the existence and deepness of the tissue. This artifact is more evident with the growing intensity of the reflected signal.
- Comet tail: it is a particular artifact of reverberation between the transducer and the reflective object and between the front and rear interface of an object (inner reverberation). Small dimensions reflective structures present very close reverberations which create a comet tail effect, that is many small parallel bands of echoes arranged transversely to the direction of the US beam. They are tighter as we get away from the element that generated them which is why the comet tail often has a triangular shape with a vertex downstream. This type of artifact is generated from the presence of gas in cavities, vessels and ducts, from calcifications of various nature, from metal catheters, plastic material and probes elements and from clips or foreign bodies.
- Mirror: a formation, placed between the transducer and a very reflective interface, determines a second reflected image. This second image will be placed downstream with respect to the interface and along the direction of the US beam. We can have an axial reflection, in which the reflective interface is nearly perpendicular to the US beam, and a non-axial reflection, in which the interface is a little curved and so it is not generated just below the US beam.

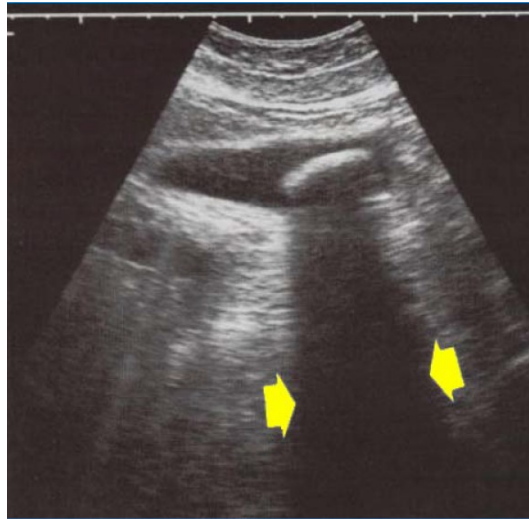


Figure 7.9. *The figure shows an example of the shadowing artifact*

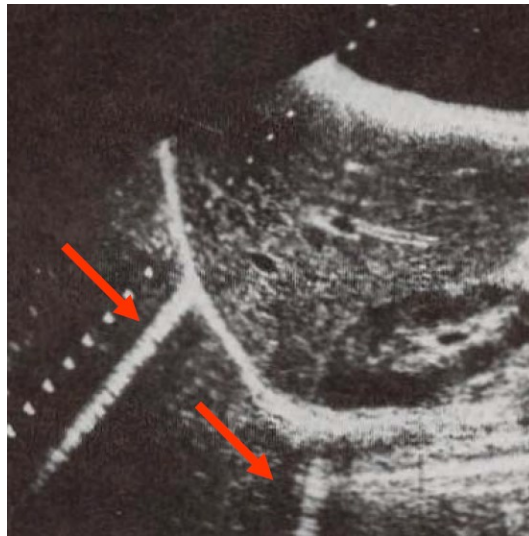


Figure 7.10. *In this figure, instead, is shown an example of the comet tail artifact*

# Chapter 8

## Materials and methods

To do “good ultrasonography” and in general to complete the protocol we use the following instruments and systems of measure:

- MicrUs EXT-1H

The firm Telemed devised an open architecture diagnostic system based on ultrasound called *micrUs Ext-1H*. It is a very flexible and versatile technology because it exploits the USB power supply, the fanless technology and can be used on PCs, tablets and smartphones. It allows the use of a wide range of multi-frequency transducers with wide bandwidth, from 2,0 to 15,0 MHz, which enables high image quality in various clinical fields: general, abdominal, obstetrical-gynaecological, small parts, musculoskeletal, urological, ultrasound-guided procedures, etc. The supported probes are linear, convex, micro convex, and endo-cavitary with a depth that goes from 2 up to 31 cm depending on the probe used and the display modes are various (including B and M mode). To use the architecture, the company provides the beamformer and wiring (usb); the user must download the software and drivers contained in the USBdrive, also provided at the time of purchase. To start the acquisition procedure you will need to connect the beamformer to the pc (via usb wire) and then connect the probe to the beamformer. Thus you are ready to start an ultrasound acquisition, the display of which will be calibrated according to the resolution of the laptop monitor.

- ECHO WAVE II scanning software

The system is driven by the ECHO WAVE II scanning software with an intuitive user interface shown in the figure 8.1. On the left side of the panel are several parameters that the user can change to adjust image quality and improve performance. The most important controls to

adjust are: scan depth, gain, TGC and focus.

First of all, the depth changes depending on the type of body region to be scanned, specifically a larger, inner area requires a greater depth value and vice versa. Greater depth can also be obtained by selecting a low value for the ultrasound probe frequency.

Secondly, gain and time gain compensation (TGC) play a key role in the reception of the signal to the probe, namely the return echo. The body tissues in fact attenuate the mechanical wave, and it is therefore essential to use the TGC parameter to compensate for the depth effect that is superimposed on the effect of the reflection coefficient when an echo arrives at the probe. Moreover the gain parameter has an effect over all return signals, it in fact act on brightness of the image acquired, which is the sum of signals coming from different depths.

Finally, the focus parameter turns out to be useful for varying the resolution in specific areas through the use of special markers. Specifically, the software allows you to choose the depth and area of focus.

After the proper captures are completed, several operations can be performed including a saving of the videos or images either in .mp4 or .avi format or other similar formats. However, it is possible to work and perform measurements both on newly collected images and on images previously saved in memory.

The software eventually allows to archive this data and create an actual report for each subject analyzed.

At least there are some parameters that the user can set. Firstly, the Dynamic Range it works on contrast, that is, the parameter changes the gray scale by increasing or decreasing gray tones. By doing so, it is possible to more accurately detail structures with different acoustic impedance that otherwise would not be distinguished from one another.

The Color map values might be set through the *Palette*, and it works on brightness and darkness of each image level. The quality of an image is based also on the noise reduction, therefore to limit it can be used two commands: *Frame averaging* and *Rejection*.

Overall there are several default configuration (Presets) which can be selected depending on the probe used and the examination to be performed. The user is able to add presets if he deems it necessary.

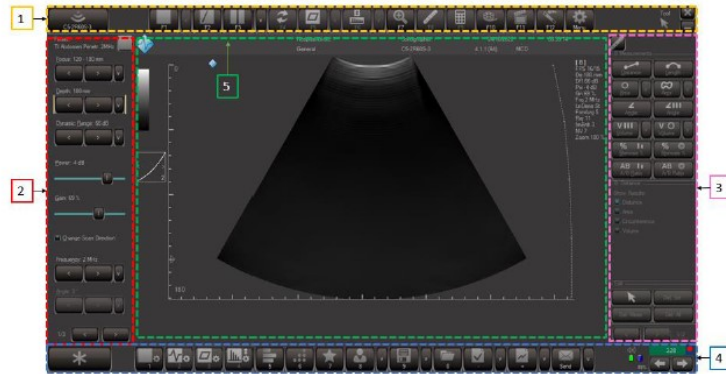


Figure 8.1. Software user interface [16]

## 8.1 Ultrasound probe

For this project, a Convex-type probe, C5-2R60S-3, manufactured by the company Telemed, was used (figure 8.2). "The crystals on the probe are S3 type and the transducer can work in the frequency range of 2-5 MHz. It has a bending radius of 65 mm and a field of view of 60°. The main applications are for abdomen, gynecology, and pediatric ultrasound". [7]



Figure 8.2. *The figure shows the Convex probe C5-2R60S-3.*

## 8.2 Impedance scale

The scale used is a Tanita brand commercial scale, model BC-730 [30]. It uses bioimpedance analysis to measure body composition by sending a safe, low-frequency signal throughout the body from the 4 electrodes placed in the base of the scale. This signal circulates through muscle tissue fluid, stopping when it finds resistance from fat tissue. This resistance, called, Bioimpedance, is calculated accurately and its results change depending on a person's gender, height and weight to give a personalised fat and body composition reading.

It is possible to use it in 'guest' mode, allowing the age, gender and height of the person to be weighed to be selected.

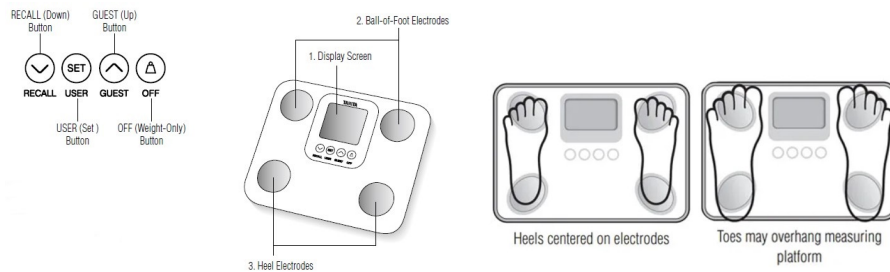


Figure 8.3. The figure shows the Tanita BC-730 scale and its settings [30]

The parameters returned are total body weight, body fat percentage, visceral fat index, muscle mass, physical index, bone mass, BMR, metabolic age and total body water. The device is powered by batteries and has 4 impedances on which the subject's feet are placed. To ensure accuracy, the manual recommends taking measurements undressed and if this is not possible to always remove the socks anyway. In our case, as it was not possible to have the candidates completely undressed, the second recommendation was followed, so the candidates were weighed barefoot. Heels must be correctly aligned with the electrodes on the measuring platform and even if the feet appear too large for the unit, accurate readings can still be obtained if the toes overhang the platform [30]. The scale has a compact design (21.6 x 26 x 3.5 cm) and the maximum user weight supported is 150 kg with an accuracy of 100 g on total body weight and 0.1% on body fat. The last two images on the right show the right placement of the feet on the four impedances placed on the surface of the scale.

### 8.3 Heart rate sensor Polar H10

During the exercise to monitoring the heart rate and the frequency of the candidates a Polar H10 heart rate sensor has been used. It is a very precise heart rate sensor that comes with the Polar Pro chest strap, and provides interference-free electrical measurement. Polar H10 connects and transfers data via Bluetooth® and ANT+™. and so it has a variety of connection possibilities with compatible sports watches, smart

watches and training apps [18]. In our study we used the ECG logger app that permits to register the entire ECG tracing in a .csv format. The plastic electrodes areas on the reverse side of the strap detect heart rate and the connector sends this heart rate signal to the receiving device (in our case a smartphone). The Polar H10 has a CR 2025 battery with a lifetime of nearly 400 h. It can operate in the following range of temperatures: -10 °C to +50 °C. For optimal detection, the belt should be positioned just below the chest and to ensure sufficient transmission range from the Polar H10 heart rate sensor to the receiving device, the device should be kept in the front.

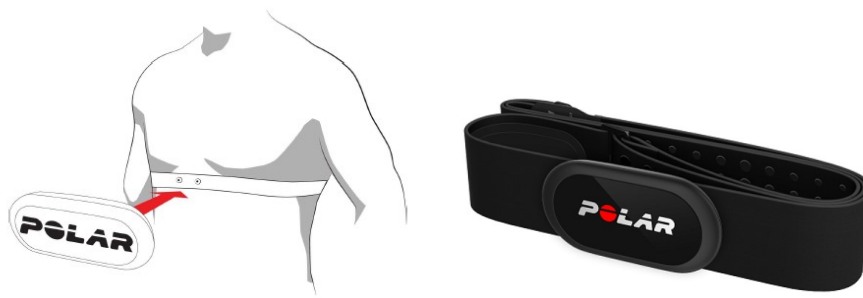


Figure 8.4. *How to dress the band correctly* [18]

## 8.4 Treadmill

A treadmill model Reharunner 02, from Chinesport S.p.A., Italy, [19] was used to exercise the candidates and thus induce sweating. The system is CE-marked, and the walking parameters can be set from the on-board computer, which allows adjustment of the belt speed and incline. Further settings can be customised from the control panel. It has a walking surface of 154 x 54 cm and supports a maximum working load of 180 kg. The device is mains-powered (220-240 V, 15 A, 50-60 Hz) and draws a maximum power of 2000 VA. The maximum permitted speed is 25 km/h, and the maximum inclination is +30% [19].



Figure 8.5. *structure and interface of the treadmill [19]*

## Chapter 9

### Test protocol execution

To evaluate the variation of diameter of the inferior vena cava after a loss of hydration, we subjected some candidates, amateur or semi-professional athletes, to a physical test to induce consistent sweating in them. First of all, some measurements were taken to obtain a baseline to be compared with subsequent measurements taken during and after the test. In particular, the candidates were weighed with the impedance scale described above, to detect body weight and percentage of total body water, they underwent an initial vena cava scan with ultrasound (video of approximately 10–15 seconds) and finally they wore the Polar H10 band to detect ECG and resting heart rate. During the test they were asked to wear sports clothing consisting of shorts and a short-sleeved shirt. The candidates were then subjected to a sustained uphill walk on the treadmill, with a speed of 5 km/h and 10 % incline as initial parameters, for 10 minutes followed by a 5-minute break during which new weight and IVC scan measurements were taken. This routine was repeated 4 times for a total of 40 minutes of exercise interspersed with the respective measurements. The speed and slope parameters were adjusted during the tests according to the candidate's sweating rate. At the end of the last task, the candidates were asked to re-hydrate with an appropriate amount of water based on the fluid lost (calculated from the weight loss measured by the scales). During re-hydration, a new ultrasound was performed to monitor the filling of the vein and every two minutes thereafter to check the change in size of the inferior vena cava following fluid replenishment. 30 candidates were tested, 14 women and 16 men of whom 20 are sportspersons. 7 athletes are volleyball players, the most represented sport in the dataset. During the examination, candidates were lying on an ultrasound couch in a supine position [22]

## 9.1 Dataset Costruction

First of all , starting from the candidates that underwent the testing protocol, a dataset was created. This dataset is shown in the graph below. It contains the information acquired from each subject such gender, age or weight, and provides an overview of the characteristics of its subjects, which will be useful when a statistical analysis is performed on the results obtained. From each subject of the dataset the following ultrasound videos have been acquired over time:

- At the starting point: baseline IVC
- In the sweating phase: IVC after 10 minutes of activity, IVC after 20 minutes of activity, IVC after 30 minutes of activity, IVC after 40 minutes of activity
- In the hydration phase: IVC immediately executed,IVC after 2 minutes, IVC after 4 minutes, IVC after 6 minutes, IVC after 10 minutes.



Figure 9.1. Dataset information:(upper right)Age,(upper left) Gender, (lower right) Weight, (lower left) Body water

After collecting data from each step of activity, it was possible to run a series of graphs showing weight trends over time and see what the trend of the subjects was. The result is shown in the following graph:

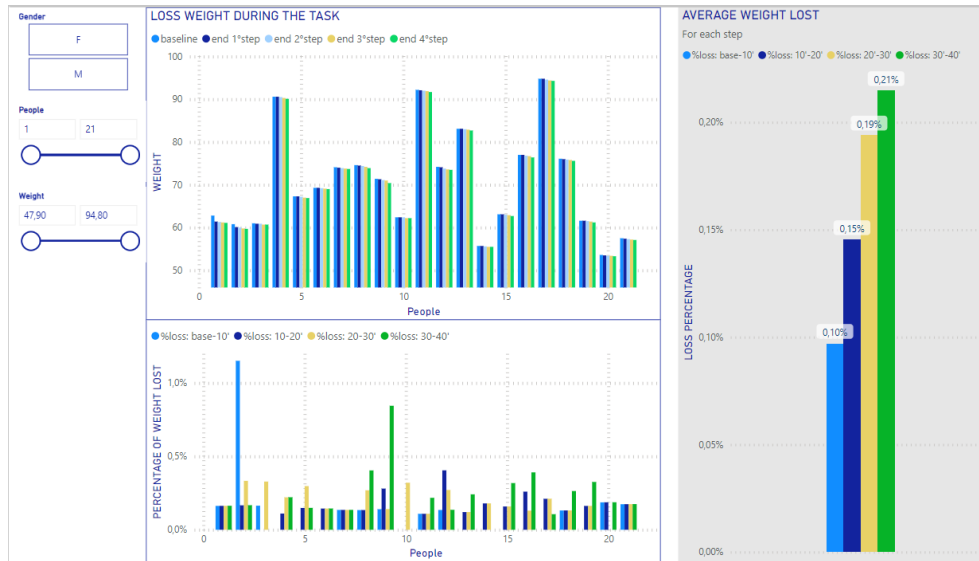


Figure 9.2. UpLeft:weight for each subject in each step, LowLeft:% of weight lost;Right:average of weight lost for each step

The above graphs are included in an extensive report, created using the Microsoft Power BI tool, which provides an overview of all the stages of the project and all the steps taken to arrive at the measurement of the variables of interest such as diameter and caval index. The final report can be found at the following link :

<https://app.powerbi.com/groups/me/reports/b8746929-0cdd-415d-9a4d-4e53aefbc0f5?experience=power-bi>

# Chapter 10

## Diameters generation

During the execution of the protocol were acquired ultrasound videos in both longitudinal and cross sections. However, after a visual check it was noticed that in cross-sectional videos the inferior vena cava was not always visible, and for this reason it was decided to do processing mainly on the vein in longitudinal section. The main purpose for which these videos were processed was to obtain a stable diameter measurement not for a single frame but for the entire duration of the acquisition, so as to provide a reliable and robust indication of this parameter. So, to reach the purpose, several steps were performed through the creation and execution of MATLAB codes. The various steps are detailed here , in each section.

## 10.1 Segmentation of the vein

To elaborate the ultrasound scan videos was used "custom-made software (implemented in MATLAB 2020a, The MathWorks, Natick, MA)" [17]. Starting from the raw video, through a manual selection of the vein border was performed an initial segmentation of the inferior vena cava. Initially was selected two high-contrast points, easily visible from the SW throughout the video; then the two edges (upper and lower) of the blood vessel were selected. [22] [17]. Finally, the last output provided to the software was the right edge of the vein. It represents the boundary of the vein tract to be segmented.

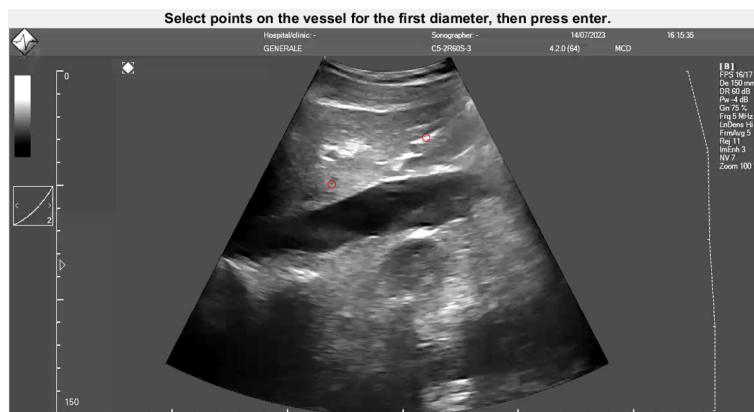


Figure 10.1. first step: the two points to do tracking.

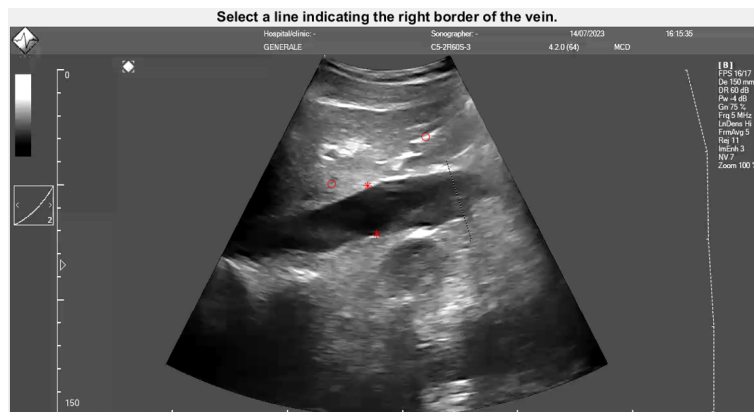


Figure 10.2. second step: upper,lower,right edges.

Each video has different duration and characteristic, from here the needs

to customize two parameters for each elaboration. In fact before starting the segmentation it was set the type of vein (longitudinal or transversal) and the Start/End frame. This last parameter allow to segment the vein deleting noise or disturb (as tissue overlapping or manual artifact generated by ultrasound probe) obtaining a clean elaboration of the data.

## 10.2 Diameter generator

For a certain number of points, managed by the user the software VIPER create the diameters, which are distributed along the entire length of the vein. To obtain the diameter measurement using the segmentation algorithm developed by VIPER, a number of lines (21 in this case) perpendicular to the vessel median was chosen. The intersection of these lines with the upper and lower edge of the IVC determines the diameter value. To establish a single diameter value, firstly a reduction of the diameters was made to the central part of the vein only, to avoid edge effects, and secondly an average of the remaining diameters was performed.

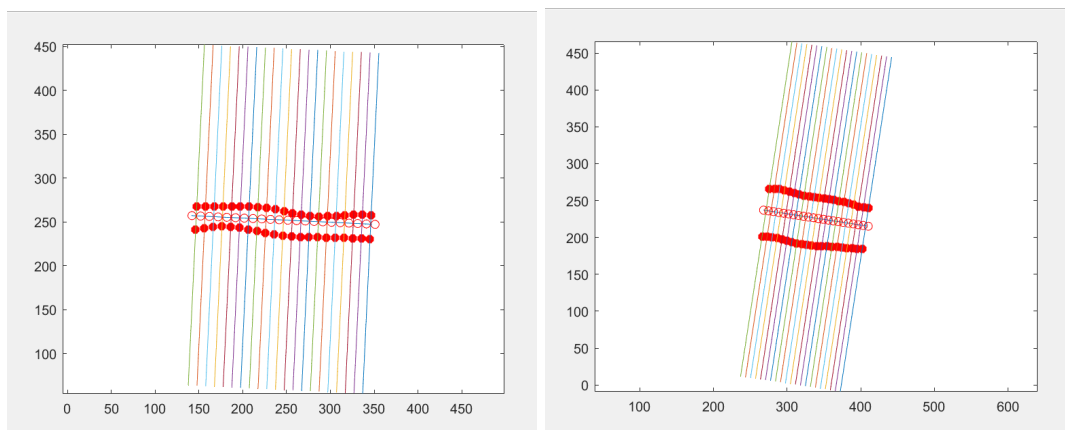


Figure 10.3. Diameters of a video recorded during dehydration (L) and hydration (R).

### 10.3 Conversion factor

The diameters calculated above return a value in pixels that must be converted to millimeters. This is essential to get practical and accurate feedback on the measurement obtained, so that it can be compared with reference values. Therefore it was evaluated the depth of each single echographic video that in the specific case was between 90 and 150, after that a different conversion factor was extracted for each depth, and the diameter in pixels was converted to mm. The values of conversion factors obtained ranged from about 0.23 to 0.28

### 10.4 Extraction of parameters

The precise segmentation of blood vessel diameter always has a physiological purpose. So, by extracting the central part of the vein using the software to avoid edge effects, the average value of the diameter of the vena cava was calculated [17]. So all the previous steps, designed to generate a diameter measurement in millimeters from an ultrasound image, are used to calculate physiological indices. Specifically these indices are the collapsibility index (or caval index CI) the respiratory caval index (RCI) and the cardiac caval index (CCI). To obtain these indices from "mean diameter" it was filtered and treated in this way: "low-pass filtered, with cut-off frequency equal to  $m_f \pm 0.5$  Hz (Chebyshev of type I, stop band starting at  $m_f + 1.5$  Hz, passband from 0 to  $m_f + 0.5$  Hz)" [17]. In particular, the most interesting parameter from a statistical point of view turned out to be the CI, which is described by the formula [23]:

$$CI = \frac{(\max(D) - \min(D))}{\max(D)} \quad (10.1)$$

These measurements were acquired over time, each time an ultrasound measurement was taken, thus: before starting, four times during physical activity, and another 4 times during hydration.

### 10.5 Normalization of diameters

In this section is shown the diameter's values for each protocol steps after a normalization. Practically it was normalized all the diameters in each instant of time respect to the first value. This approach allows

you immediately distinguish the data in the two main phases: hydration and dehydration. In fact, normalization to zero the first value clearly highlights values greater than zero (greater peaks during hydration) and lower values during dehydration. The lowest value is found at the end of the activity. The normalization it was necessary because of high inter-subject variability in vena cava diameter. This makes it possible to make the values comparable to each other.

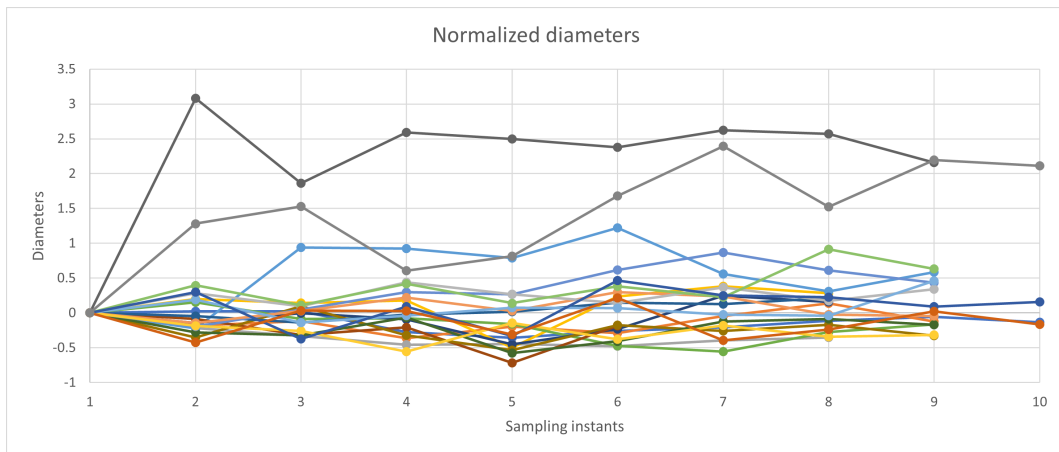


Figure 10.4. Normalized diameters respect to the first value

To clarify the general trend and to see if the trend correspond to the initial hypothesis, it was we averaged the diameters of all subjects for each time instant thus obtaining a general trend like that ,shown in figure:

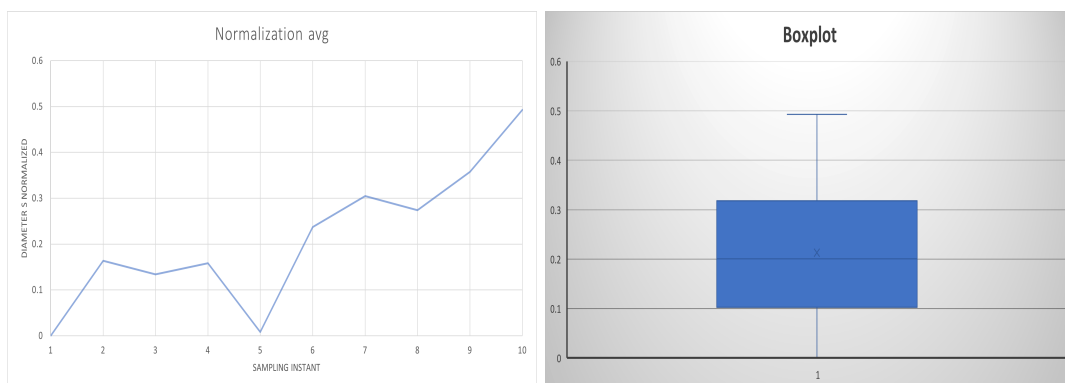


Figure 10.5. Trend and boxplot for diameters normalized

# Chapter 11

## Results and graphs

The results confirm the hypothesis that after an exercise activity the diameter of IVC tends to reduce, while after a recovery (hydration) the vein return to the initial dimension. Contrary to what we might have thought at the beginning of our project, before we even acquired all the data, we do not have a complete decrease during dehydration and a complete growth during hydration, but they show the trend in [11.1](#)

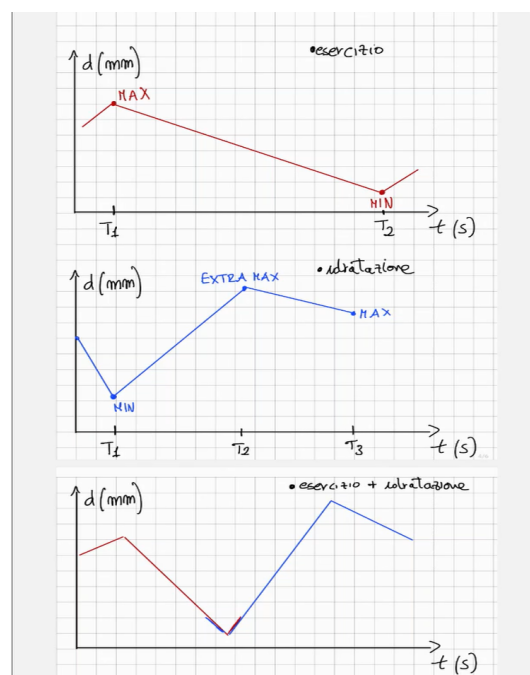


Figure 11.1. The figure shows the real trend of the IVC diameter. At the top we can see the trend of dehydration, in the middle the trend of hydration and at the bottom the two trends come together.

As we can see, during the dehydration phase some patients need a phase called 'warm up' in which the vein diameter grows to a maximum and then begins to decrease in diameter. Similarly during the hydration phase the diameter grows to a point above the maximum value found during the dehydration phase and then stabilizes around this value.

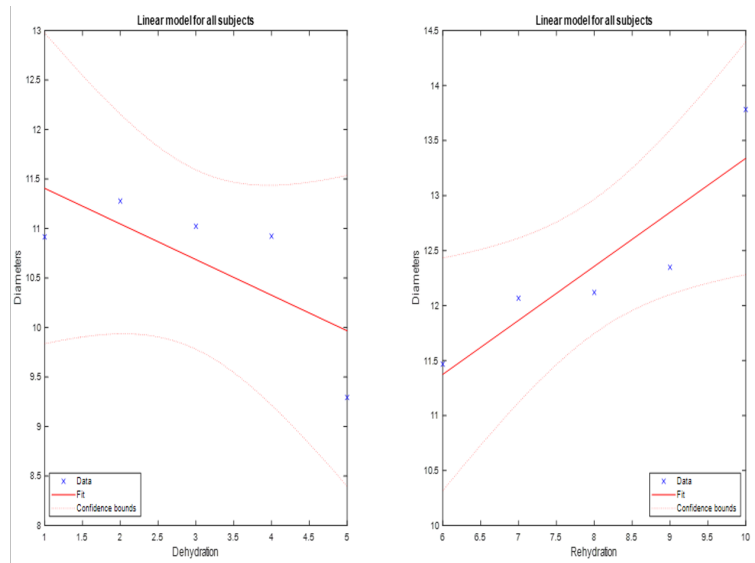


Figure 11.2. Here are shown the linear model of the entire data-set averaged.

In general, however, we can say, through the development of a linear model that interpolates the data from the entire data-set averaged, that the trends of the initial assumptions are maintained and that we therefore have a descending phase during dehydration and a growing phase during hydration (as shown in the figure 11.2).

However, not all patients in the dataset show the same behavior. In fact, the linear model was applied to each patient, and some of them showed a behavior described as 'peculiar'. As a demonstration, we show in the image below a couple of examples of abnormal behavior. The figure outcome is an interpolation of the vena cava diameter data in two phases: during dehydration and during hydration.

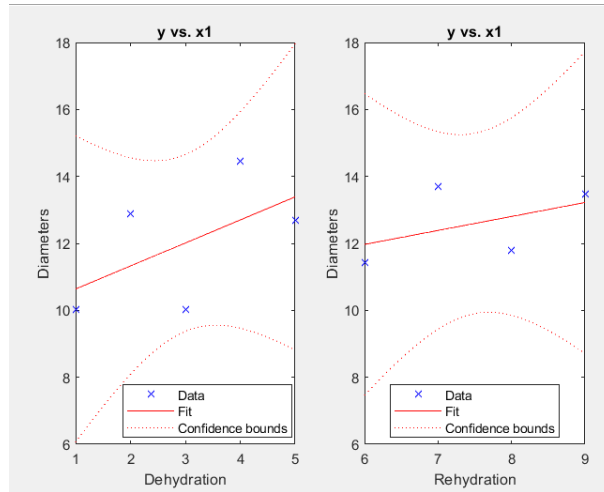


Figure 11.3. In this figure we can observe a particular behavior for the dehydration phase.

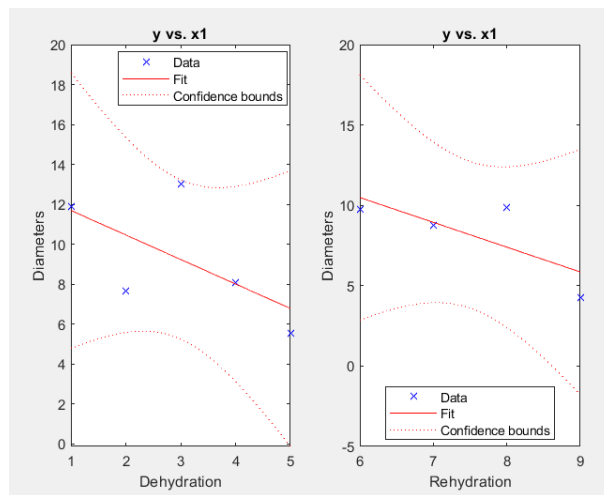


Figure 11.4. In this figure we can observe a particular behavior for the hydration phase.

For some subject defined "particular" the trend was not as expected, and this may be due to various factors, such as the need for the vein to warm up before physical activity; absorbing blood from the body to make up for the effort, before releasing it into the tissues.

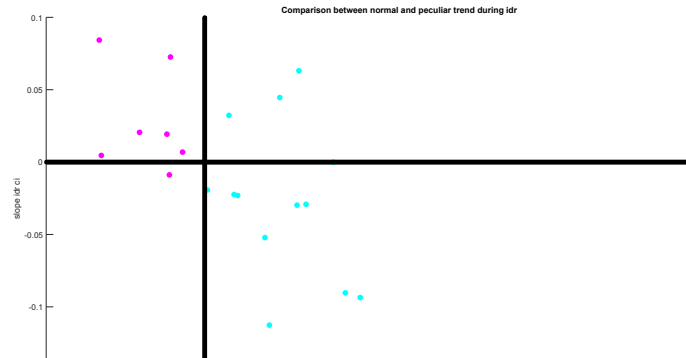


Figure 11.5. Scatter plot of CI vs Diameter between particular and normal subjects

Unfortunately, for statistical purposes, no significant correlations emerged between the subjects called "particulars", this may mean that their behavior is subjective and varies based on a multiplicity of factors that may not be observable through our study. But in general once the correlation between these two populations was observed, the spectrum of analysis was broadened focusing on the entire group. The two graphs

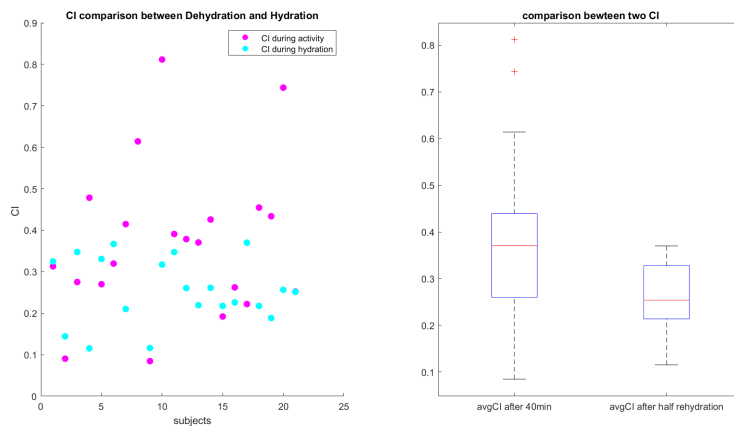


Figure 11.6. Scatter plot of two different CI for all dataset (L) and boxplot with significance (R)

represent two indicative caval index during the two phases of dehydration and hydration. One of these CI is taken after 40 minutes, when the vein is most empty; while the other measure involve the CI after half hydration, when the highest peak of diameter is measured. Following the statistical significance found among the parameters shown in the graph, the main focus was explored. That is, the presence of differences between sporting and non-sporting subjects was tested.

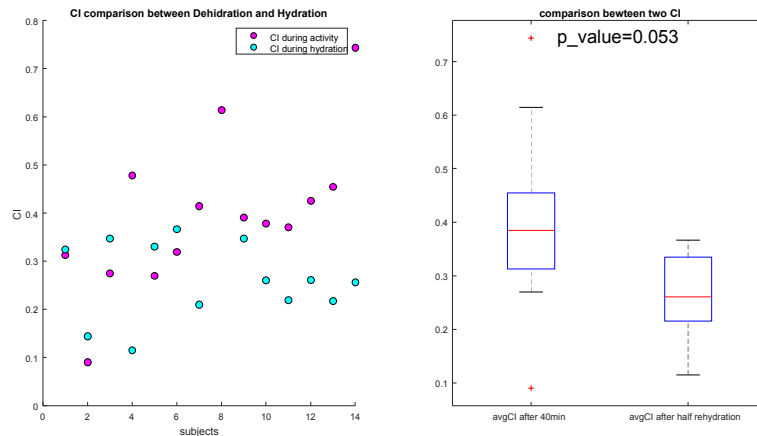


Figure 11.7. *This chart is for the 14 sports subjects. The values of the two CIs are always compared. NB for athletes there is significance between before and after hydration. For non-sportsmen there is no significance and we have not represented them*

A significant result has been achieved. For the category of sports subjects there remains a statistical difference between the analyzed parameters, while for non-sports candidates this difference is not statistically significant

## 11.1 Statistical test

The study of significant parameters to examine the reasons for the decrease and growth of diameter in the two phases were investigated through various statistical tests. To choose which tests to perform, a check on the normality (Gaussian curve) of the variables to be analyzed was carried out by means of 10 tests including Shapiro-Wilk, Shapiro France and Kolmogorov. The result obtained, namely the confirmation of the Gaussian curve for the tested variables led to the use of a parametric statistic and the following tests: Anova, t-test, rankum. The

following section will illustrate some tables highlighting the tests performed whether they are significant or not. The categories tested were different, as noted in the section 11. Firstly the entire dataset, and after the two subgroups: "Athletes" and "Not athletes". In addition it is important emphasize that in accordance with what is observed in the figures 11.3 and 11.4 the test execution involved the two subcategories of subjects particular for hydration phase and dehydration phase.

Test	Dataset	Comparison	p_value	Signif.
Ranksum	Sport vs Non Sport	Delta heart rate	0.1352	no
Ranksum	Sport	CI exercise and during hydration	0.0053	yes
Ranksum	Non Sport	CI exercise and during hydration	0.6200	no
Ranksum	Entire dataset	CI exercise and during hydration	0.0110	yes
Ranksum	NormVpartic (dehydr)	Vein emptying during effort	0.2006	no
Ranksum	NormVpartic (hydr)	Delta heart rate	0.0858	no
Anova 1	Entire dataset	Avg diam during hydr V Gender	0.1534	no
AnovaN	Entire dataset	Avg diam during hydr V Gender	0.3053	no
AnovaN	Entire dataset	Avg diam during hydration V Age	0.5116	no
AnovaN	Entire dataset	Avg diam during hydration V Sport	0.9661	no
AnovaN	Entire dataset	Avg diam during dehydr V Gender	0.5802	no
AnovaN	Entire dataset	Avg diam during dehydr V Age	0.5423	no
AnovaN	Entire dataset	Avg diam during dehydr V Sport	0.7204	no
t-test2	Sport vs Non Sport	Avg diameter hydration	0.4671	no

Table 11.1. Test executed

Legend:

- avg= average
- CI= caval index
- dehydr= dehydration phase
- diam= diameter
- hydr= hydration phase
- Norm= normal
- part= particular
- Signif= significance

In the table above the most relevant tests performed on the various dataset are included. It can be seen that only two tests were significant

and have been reported in the [11](#) section. It is necessary to point out some aspects:

- Delta heart rate is the difference of heart rate between the beginning and end of the effort
- When the caval index comparison appears, we refer to the difference in CI between the end of exercise and about halfway through hydration, when the maximum peak in diameter is witnessed

## 11.2 Conclusions

At the end of our project we can say that our hypotheses were only partially confirmed. In fact, initially we expected to have a complete decrease during the exercise phase, and thus dehydration, and a complete increase instead during the hydration phase. As shown in the results the trend is more complex although the general trend is in line with the hypothesis made, that is, decrease during dehydration and growth during hydration.

The overall normalization, derived from the average of all diameters for each instant, demonstrates this statement well. From the figure 10.5 we can indeed see the initial warm-up phase, the descent to the minimum at the end of the exercise, and the rise during hydration. In addition to this, the importance of the caval index was confirmed as a key parameter, useful in attesting to diameter variability and making statistically relevant distinctions on the patients under study.

This parameter allowed us, in addition to attesting whether the candidates were fluid-deficient, to observe different behavior between athletic and nonathletic subjects. In fact, the vena cava of sports subjects showed greater adaptability to external changes, reacting more quickly to the reintroduction of fluids into the body respect to the other group of subjects.

Certainly this thesis project opens the door to new developments and insights. For example, it would certainly be useful to increase the duration of the exercise phase in order to observe the decreasing trend in this phase even more surely. The use of a more uniform candidate dataset could also contribute to the further improvement of the results and could give rise to new significances that, with a heterogeneous dataset such as the one in this thesis project, did not arise from the analyses performed. also add the possible direction for future works, extending the thesis work.

# Bibliography

- [1] <https://www.viper.srl/>.
- [2] <https://youtu.be/mbHcGi7D7mg?t=2>.
- [3] <https://youtu.be/qHWLFFxtGn8>.
- [4] <https://www.telemedultrasound.com/products/>.
- [5] <https://radiologykey.com/vessels/>.
- [6] <https://youtu.be/McUUFvnFuJU?t=18>.
- [7] <https://www.medicalexpo.it/prod/telemed-medical-systems/product-70298-718259.html>.
- [8] Stefano Albani, Luca Mesin, Silvestro Roatta, Antonio De Luca, Alberto Giannoni, Davide Stolfo, Lorenza Biava, Caterina Bonino, Laura Contu, Elisa Pelloni, et al. Inferior vena cava edge tracking echocardiography: a promising tool with applications in multiple clinical settings. *Diagnostics*, 12(2):427, 2022.
- [9] Lindsay B Baker. Sweating rate and sweat sodium concentration in athletes: a review of methodology and intra/interindividual variability. *Sports Medicine*, 47:111–128, 2017.
- [10] Melissa C Caughey, Carla A Sueta, Sally C Stearns, Amil M Shah, Wayne D Rosamond, and Patricia P Chang. Recurrent acute decompensated heart failure admissions for patients with reduced versus preserved ejection fraction (from the atherosclerosis risk in communities study). *The American journal of cardiology*, 122(1):108–114, 2018.
- [11] Samuel N Chevront and Michael N Sawka. Hydration assessment of athletes. *CHINESE JOURNAL OF SPORTS MEDICINE*, 25(2):238, 2006.
- [12] Christopher Cook, Graham Cole, Perviz Asaria, Richard Jabbour, and Darrel P Francis. The annual global economic burden of heart failure. *International journal of cardiology*, 171(3):368–376, 2014.
- [13] Jose Curbelo, Maria Aguilera, Pablo Rodriguez-Cortes, Paloma Gil-Martinez, and Carmen Suarez Fernandez. Usefulness of inferior vena cava ultrasonography in outpatients with chronic heart failure. *Clinical cardiology*, 41(4):510–517, 2018.
- [14] Agarwal Dipti, Zachary Soucy, Alok Surana, and Subhash Chandra.

- Role of inferior vena cava diameter in assessment of volume status: a meta-analysis. *The American journal of emergency medicine*, 30(8):1414–1419, 2012.
- [15] R.Maggi E.Carbone, G.Aicardi. *Fisiologia, dalle molecole ai sistemi integrati*. EdISES, 2018.
- [16] *EchoWavell-Manuale-Utente*.
- [17] Leonardo Ermini, Stefano Seddone, Piero Policastro, Luca Mesin, Paolo Pasquero, and Silvestro Roatta. The cardiac caval index: Improving noninvasive assessment of cardiac preload. *Journal of Ultrasound in Medicine*, 41(9):2247–2258, 2022.
- [18] *Polar h10 user manual*.
- [19] *REHARUNNER 02 PC*.
- [20] Gianni Losano, Raffaella Rastaldo, and Amedeo Chiribiri. *Fisiologia cardiovascolare: un approccio integrato*. River Publishers, 2013.
- [21] Luca Mesin, Stefano Albani, Piero Policastro, Paolo Pasquero, Massimo Porta, Chiara Melchiorri, Gianluca Leonardi, Carlo Albera, Paolo Scacciatella, Pierpaolo Pellicori, et al. Assessment of phasic changes of vascular size by automated edge tracking—state of the art and clinical perspectives. *Frontiers in Cardiovascular Medicine*, 8:775635, 2022.
- [22] Luca Mesin, Tatiana Giovinazzo, Simone D’Alessandro, Silvestro Roatta, Alessandro Raviolo, Flavia Chiacchiarini, Massimo Porta, and Paolo Pasquero. Improved repeatability of the estimation of pulsatility of inferior vena cava. *Ultrasound in Medicine & Biology*, 45(10):2830–2843, 2019.
- [23] Luca Mesin, Paolo Pasquero, Stefano Albani, Massimo Porta, and Silvestro Roatta. Semi-automated tracking and continuous monitoring of inferior vena cava diameter in simulated and experimental ultrasound imaging. *Ultrasound in Medicine & Biology*, 41(3):845–857, 2015.
- [24] Kensuke Nakamura, Makoto Tomida, Takehiro Ando, Kon Sen, Ryota Inokuchi, Etsuko Kobayashi, Susumu Nakajima, Ichiro Sakuma, and Naoki Yahagi. Cardiac variation of inferior vena cava: new concept in the evaluation of intravascular blood volume. *Journal of Medical Ultrasonics*, 40:205–209, 2013.
- [25] Daniele Orso, Nicola Guglielmo, Nicola Federici, Francesco Cugini, Alessio Ban, Filippo Mearelli, and Roberto Copetti. Accuracy of the caval index and the expiratory diameter of the inferior vena cava for the diagnosis of dehydration in elderly. *Journal of ultrasound*, 19:203–209, 2016.
- [26] Susannah J Patey and James P Corcoran. Physics of ultrasound. *Anaesthesia & Intensive Care Medicine*, 22(1):58–63, 2021.

- [27] Aurora Giambartolomei; Michela Pieragostini. Test of a new ultrasound system for monitoring the edges of the inferior vena cava. Master's thesis, Politecnico di Torino, Torino, 2023.
- [28] Andrea Poli and Francesco Visioli. Idratazione e salute.
- [29] Cindy L Stanfield, William J Germann, Mary Jane Niles, and Joseph G Cannon. *Principles of human physiology*. Benjamin Cummings London, 2011.
- [30] Tanita. *Tanita BC-730 Scale*.
- [31] Anna L Waterbrook, Amish Shah, Elisabeth Jannicky, Uwe Stolz, Randy P Cohen, Austin Gross, and Srikar Adhikari. Sonographic inferior vena cava measurements to assess hydration status in college football players during preseason camp. *Journal of Ultrasound in Medicine*, 34(2):239–245, 2015.
- [32] G.C. Balboni; A. Bastianini; E. Brizzi; L. Comparini; G. Filogamo; P. Fusaroli; G. Giordano-Lanza; C.E. Grossi; F.A. Manzoli; G. Marinozzi; A. Miani; P. Motta; E. Nesci; G.E. Orlandini; A. Passaponti; E. Reale; A. Ruggeri; A. Santoro; D. Zaccherò. *Anatomia Umana I*. edi-ermes, Milano, MI, 1984.
- [33] Bojan Knap. «Hydration and Physical Activity». In: *Res Inves Sports Med* 7(4) (Apr. 2021).

# List of Tables

5.1	<i>Estimation of quantity of fluids lost every day.</i>	23
6.1	<i>Rate of absorption of tissues</i>	26
6.2	<i>Density and acoustic impedance of air, water and biological tissues with propagation rate of US in them.</i>	27
11.1	<i>Test executed</i>	61

# List of Figures

1.1	<i>The two segmentations of the IVC: longitudinal(L)and transversal(R)</i> . . . . .	6
1.2	<i>[1]</i> . . . . .	6
2.1	<i>The figure shows the circulatory system and its major vessels</i> . . . . .	10
2.2	<i>Curve volume-pressure [21]</i> . . . . .	12
2.3	<i>Structure of the blood vessels [2]</i> . . . . .	13
3.1	<i>Structure of respiratory system. Upper airway and the tract that includes the lungs and the conduction and breathing zones [15]</i> . . . . .	17
3.2	<i>Parameters of conduction and respiratory zones [15]</i> . . . . .	17
3.3	<i>The figure shows changes of the intra-alveolar pressure and of the respiratory volume during inspiration and expiration [29]</i> . . . . .	18
4.1	<i>The anatomical position of the IVC from the frontal plane and transversal plane [3]</i> . . . . .	20
6.1	<i>The figure describes a wave propagating from material 1 to material 2. At the interface, part of the wave is transmitted to material 2 with different angle (f angle) and part is reflected (r angle) at the same angle to the normal [26]</i> . . . . .	27
7.1	<i>Ultrasound scanner blocks diagram</i> . . . . .	29
7.2	<i>The figure shows the geometry of a US beam and demonstrate the necessity of the focusing process.</i> . . . . .	32
7.3	<i>The figure shows the field of a real probe and its three resolution directions: axial, lateral and in elevation.</i> . . . . .	33
7.4	<i>The probe used for the acquisitions [4]</i> . . . . .	34
7.5	<i>The images show the orientation of vein according to our probe position [5]</i> . . . . .	35

7.6	<i>The upper image [6] show the indicator orientation. The lower image highlights the correspondence of indicator with the body region visualised on display</i>	36
7.7	<i>The upper image [6] show the indicator orientation cranio-caudal direction. The lower image highlights the correspondence of indicator with the body region visualised on display</i>	37
7.8	<i>Two acquisitions with SW by Telemed [16]</i>	38
7.9	<i>The figure shows an example of the shadowing artifact</i>	40
7.10	<i>In this figure, instead, is shown an example of the comet tail artifact</i>	40
8.1	<i>Software user interface [16]</i>	43
8.2	<i>The figure shows the Convex probe C5-2R60S-3.</i>	44
8.3	<i>The figure shows the Tanita BC-730 scale and its settings [30]</i>	45
8.4	<i>How to dress the band correctly [18]</i>	46
8.5	<i>tructure and interface of the treadmill [19]</i>	47
9.1	<i>Dataset information: (upper right) Age, (upper left) Gender, (lower right) Weight, (lower left) Body water</i>	49
9.2	<i>UpLeft:weight for each subject in each step, LowLeft:% of weight lost;Right:average of weight lost for each step</i>	50
10.1	<i>first step: the two points to do tracking.</i>	52
10.2	<i>second step: upper,lower,right edges.</i>	52
10.3	<i>Diameters of a video recorded during dehydration (L) and hydration (R).</i>	53
10.4	<i>Normalized diameters respect to the first value</i>	55
10.5	<i>Trend and boxplot for diameters normalized</i>	55
11.1	<i>The figure shows the real trend of the IVC diameter. At the top we can see the trend of dehydration, in the middle the trend of hydration and at the bottom the two trends come together.</i>	56
11.2	<i>Here are shown the linear model of the entire data-set averaged.</i>	57
11.3	<i>In this figure we can observe a particular behavior for the dehydration phase.</i>	58
11.4	<i>In this figure we can observe a particular behavior for the hydration phase.</i>	58
11.5	<i>Scatter plot of CI vs Diameter between particular and normal subjects</i>	59

11.6	Scatter plot of two different CI for all dataset (L) and box-plot with significance (R) . . . . .	59
11.7	This chart is for the 14 sports subjects. The values of the two CIs are always compared. NB for athletes there is significance between before and after hydration. For non-sportsmen there is no significance and we have not represented them . . . . .	60